

University of Nevada, Reno

**Explore the Dosimetric Relationship Between Intake of Chemical
Contaminants and Their Occurrence in Blood and Urine**

A thesis submitted in partial fulfillment of the requirements
for the degree of Master of Science in Environmental Sciences and Health

by

Amy Katharine Olsen

Dr. Li Li/Thesis Advisor

December, 2023



THE GRADUATE SCHOOL

We recommend that the thesis
prepared under our supervision by

AMY K. OLSEN

entitled

**Explore the Dosimetric Relationship Between Intake of
Chemical Contaminants and Their Occurrence in Blood and
Urine**

be accepted in partial fulfillment of the
requirements for the degree of

MASTER OF SCIENCE

Li Li, Ph.D.
Advisor

Dingsheng Li, Ph.D.
Committee Member

Yeongkwon Son, Ph.D.
Graduate School Representative

Markus Kemmelmeier, Ph.D., Dean
Graduate School

December, 2023

General Abstract:

The dosimetric relationship between the human intake of a chemical contaminant (an “external dose”) and its concentrations in bodily fluids such as blood and urine (related to an “internal dose”), often characterized by a dose-to-concentration ratio, has critical applications in exposure science, toxicology, and risk assessment, especially in the “new approach methods” era. However, there is a lack of a mechanistic, systematic understanding of how such a dosimetric relationship depends on fundamental chemical properties, such as partition coefficients and biotransformation half-lives. Here, we investigate this issue using a well-evaluated toxicokinetic model, which links external and internal doses by quantifying the absorption and elimination of chemicals. Results are visualized in a series of chemical partitioning space plots, whereby a chemical’s dose-to-concentration ratio can be approximately predicted based on its partitioning between air, water, and octanol phases. Our results indicate that when taken in equal doses, chemicals with low volatility and moderate to high hydrophobicity exhibit the highest concentrations in blood, and chemicals undergoing significant biotransformation tend to exhibit lower concentrations in comparison to their counterparts undergoing negligible biotransformation but possessing similar partitioning properties. Chemicals with high hydrophilicity have the highest concentrations in urine. Such revealed property dependence is similar for both adults and children, and for individuals with normal body weights and with obesity. Overall, insights gained from this study are important in predicting blood and urinary concentrations from exposure information and in determining the exposure rate that produces the blood or urinary concentrations observed in biomonitoring studies.

Dedication:

I would like to dedicate this work to my parents, whose support and guidance has made
all this possible.

Acknowledgments:

First, I would like to acknowledge the financial support from the U.S. Environmental Protection Agency's Science to Achieve Results program (STAR; no. RD840209) that has laid the groundwork for me to be able to take part in this endeavor.

I would also like to thank Zhizhen Zhang for her assistance in calculating the properties of chemicals used for model evaluation as well as all members of HEAT for their support during the refinement of this work.

Additionally, I would like to thank my advisor, Dr. Li Li, and the members of my committee for their guidance and support in getting me this far.

Lastly, I would like to thank my parents (Mark and Luana Olsen), my brother (Dane Olsen), Andrew Sundquist, Kellisa Shirane, and Christian Suarez for their linguistic assistance during the preparation of this manuscript, constant prayer and encouragement throughout my studies, and unwavering belief in my abilities to conquer what lies ahead.

Table of Contents:

General Abstract.....	i
Dedication.....	ii
Acknowledgments.....	iii
Table of Contents.....	iv
List of Tables.....	vi
List of Figures.....	vii
List of Abbreviations.....	ix
1 Introduction.....	1
2 Methods.....	5
2.1 Define the dose-to-concentration ratio.....	5
2.2 Simulations of DCRs on the PROTEX model.....	7
2.3 Investigation into the impacts of chemical properties.....	10
2.4 Calculation of chemical properties for model performance evaluation.....	11
3 Results and Discussion.....	12
3.1 Evaluation of the model performance.....	13
3.2 Occurrence of perfectly persistent organic chemicals in the blood	18
3.3 Occurrence of liable organic chemicals in blood and urine.....	24
3.4 Impacts of physiological factors on the dose-to-concentration ratio.....	25
4 Implications and Limitations.....	28
References.....	32
Appendices.....	38
Appendix 1 – Description of the PROTEX’s exposure and toxicokinetic module used in this work	38
Appendix 2 – Quantification of chemical elimination from the human body.....	39

Appendix 3 – Calculation of blood and urine concentrations of chemicals.....	41
Appendix 4 – Quantification of intestinal and respiratory absorption efficiencies.....	42
Appendix 5 – Table A.1: Comparison of modeled dose-to-concentration ratios (DCRs, in L/d) with DCRs calculated based on literature-reported data.....	43
Appendix 6 – Figure A.1: The relationship between the model’s residual (namely the difference between predicted and measured half-lives) and chemical properties DAW = Air-water distribution coefficient; DOA = Octanol-air distribution coefficient; HL = human biotransformation half-life.....	46
Appendix 7 – Figure A.2: Chemical partitioning space illustrating the ratio of intake dose to blood concentration for ingestion (Panel a) and inhalation (Panel b), as well as the ratio of intake dose to urinary concentration for ingestion (Panel c) and inhalation (Panel d), of hypothetical perfectly persistent chemicals (molar mass = 300 g/mol), by an archetypal 3-year-old female American child. Chemicals are arranged by log KAW and log KOA; diagonals represent chemicals with equal log KOW.....	47
Appendix 8 – Figure A.3: Chemical partitioning space illustrating the ratio of intake dose to blood concentration for ingestion (Panel a) and inhalation (Panel b), as well as the ratio of intake dose to urinary concentration for ingestion (Panel c) and inhalation (Panel d), of hypothetical perfectly persistent chemicals (molar mass = 300 g/mol), by a 25-year-old female American who has twice bodyweight of an average female American. Chemicals are arranged by log KAW and log KOA; diagonals represent chemicals with equal log KOW.....	48

List of Tables

Table A.1: Comparison of modeled dose-to-concentration ratios (DCRs, in L/d) with DCRs calculated based on literature-reported data.....	43
---	----

List of Figures

Figure 1: Schematic overview of PROTEX’s human exposure and toxicokinetic module. It calculates chemical concentrations in blood and urine resulting from a single unit dose of chemical intake by mechanistically quantifying absorption and elimination processes as functions of chemical properties (partition coefficients between octanol, air, and water and biotransformation half-life) and physiological factors (such as functions of age, sex, and bodyweight). For illustration purposes, the model is parameterized to represent a 25 year old archetypal female American (Results for Sections 3.1 through 3.3). Additional computations are conducted for a 3 year old female child and an obese individual with a bodyweight and fat weight twice that of the American average (Results for Section 3.4).....7

Figure 2: PROTEX-predicted efficiencies through intestinal (Panel a) and respiratory (Panel b) absorption (contour diagrams) as a function of $\log K_{AW}$ and $\log K_{OA}$ in comparison with literature-reported measurements (colored dots). Comparison between the modeled and literature-reported total elimination half-lives (Panel c). PROTEX-predicted half-lives for combined non-biotransformation elimination processes (exhalation, egestion, urination, and percutaneous excretion considered in this work) and the dominant processes of elimination (Panel d).....12

Figure 3: Chemical partitioning space illustrating the ratio of intake dose to blood concentration (DCR_{blood}) for ingestion (Panel a) and inhalation (Panel b) as well as the ratio of intake dose to urinary concentration (DCR_{urine}) for ingestion (Panel c) and inhalation (Panel d) of **hypothetical perfectly persistent chemicals** (molar mass = 300 g/mol) by an archetypal 25 year old female American. Chemicals are arranged by $\log K_{AW}$ and $\log K_{OA}$; diagonals represent chemicals with equal $\log K_{OW}$. Illustrative chemicals are marked based on their $\log K_{AW}$ and $\log K_{OA}$: PCB = polychlorinated biphenyl; PBDE = polybrominated diphenyl ether, D5 = decamethylcyclopentasiloxane (cyclic volatile methyl siloxane), DTDP = ditridecyl phthalate, TCE = trichloroethylene, and TMP = tris(methyl) phosphate.....18

Figure 4: Chemical partitioning space illustrating the ratio of intake dose to blood concentration (DCR_{blood}) for ingestion (Panel a) and inhalation (Panel b), as well as the ratio of intake dose to urinary concentration (DCR_{urine}) for ingestion (Panel c) and inhalation (Panel d), of chemicals (molar mass = 300 g/mol) with a **human whole-body biotransformation half-life of 2 days**, by an archetypal 25-year-old female American. Chemicals are arranged by $\log K_{AW}$ and $\log K_{OA}$; diagonals represent chemicals with equal $\log K_{OW}$23

Figure A.1: The relationship between the model’s residual (namely the difference between predicted and measured half-lives) and chemical properties D_{AW} = Air-water distribution coefficient; D_{OA} = Octanol-air distribution coefficient; HL = human biotransformation half-life.....46

Figure A.2: Chemical partitioning space illustrating the ratio of intake dose to blood

concentration for ingestion (Panel a) and inhalation (Panel b), as well as the ratio of intake dose to urinary concentration for ingestion (Panel c) and inhalation (Panel d), of hypothetical perfectly persistent chemicals (molar mass = 300 g/mol), by an archetypal 3-year-old female American child. Chemicals are arranged by $\log K_{AW}$ and $\log K_{OA}$; diagonals represent chemicals with equal $\log K_{OW}$47

Figure A.3: Chemical partitioning space illustrating the ratio of intake dose to blood concentration for ingestion (Panel a) and inhalation (Panel b), as well as the ratio of intake dose to urinary concentration for ingestion (Panel c) and inhalation (Panel d), of hypothetical perfectly persistent chemicals (molar mass = 300 g/mol), by a 25-year-old female American who has twice bodyweight of an average female American. Chemicals are arranged by $\log K_{AW}$ and $\log K_{OA}$; diagonals represent chemicals with equal $\log K_{OW}$48

List of Abbreviations

Abs	Absorption
AE	Absorption Efficiency
B	Biotransformation
BEs	Biomonitoring Equivalents
BV _{eff}	“Effective” Body Volume
C _B	Blood Concentration
CORR _{E,age}	Corrected Reduced Metabolism Capability
C _U	Urinary Concentration
D5	Decamethylcyclopentasiloxane (Cyclic Volatile Methyl Siloxane)
D	Dermal
D _{AW}	Air-Water Distribution Coefficient
D _{B,age}	Hepatic Biotransformation of Chemical for a Certain Age
DCR	Dose-to-Concentration Ratio
DCR _{blood}	Dose-to-Blood Ratio
DCR _{urine}	Dose-to-Urine Ratio
D _{E,age}	Elimination Through Egestion for a Certain Age
D _{OA}	Octanol-Air Distribution Coefficient
D _{P,age}	Elimination Through Percutaneous Lipid Excretion for a Certain Age
D _{R,age}	Elimination Through Exhalation for a Certain Age
DTDP	Ditridecyl Phthalate
D _{U,age}	Elimination Through Urination for a Certain Age
E	Egestion
Elim	Elimination
<i>f</i>	Chemical Fugacity in the Human Body
<i>f_{ub}</i>	Protein-unbound Fraction of Chemicals
<i>f_{reabs}</i>	Renal Tubular Reabsorption
GFR _{age,weight}	Renal Clearance by Glomerular Filtration
G-PBTK	Generic Physiologically Based Toxicokinetic Model
HL _{human}	Biotransformation Half-life
HTTK	High-Throughput Toxicokinetic Model
IFS-QSAR	pp-LFERs with Abraham solute descriptors computed by the Iterative Fragment Selection
ING	Ingestion
INH	Inhalation
K _{aw}	Air-Water Partition Coefficient
K _{oa}	Octanol-Air Partition Coefficient
K _{ow}	Octanol-Water Partition Coefficient
M _{body}	Total Amount of Chemical within the Human Body
NHANES	National Health and Nutrition Examination Survey

$N_{U,age}$	Chemical Flow Excreted by Elimination
OPERA	OPEn structure-activity/property Relationship App
P	Percutaneous
PBDE	Polybrominated Diphenyl Ether
PCB	Polychlorinated Biphenyl
POD	Point of Departure
pp-LFERs	Poly Parameter Linear Free Energy Relationships
PROTEX	PROduction-To-EXposure
QSARINS-Chem	QSAR-INsubria-Chem
R	Exhalation
R_{age}	Urine Flow
$R_{desquamation,age}$	Rate of Skin Desquamation
RfD	Reference Dose
$R_{food,age,weight}$	Rate of Food Ingestion
RMSE	Root-Mean-Square Deviation
$R_{respiration,age,weight}$	Rate of Respiration
spLFERs	Single-parameter Linear Free Energy Relationships
TCE	Trichloroethylene
TMP	Tris(methyl) Phosphate
U	Urination
Z_{air}	Fugacity Capacity of the Exhaled Air
Z_{blood}	Fugacity Capacity of Blood
Z_{Body}	Fugacity Capacity of the Human Body
Z_{feces}	Fugacity Capacity of Human Feces
Z_{nlipid}	Fugacity Capacity of Neutral Storage Lipids
Z_{plipid}	Fugacity Capacity of Phospholipids
$Z_{protein}$	Fugacity Capacity of Proteins
Z_{skin}	Fugacity Capacity of the Skin
Z_{water}	Fugacity Capacity of Water

1. Introduction:

Every day, humans around the world are exposed to a variety of chemicals emitted from chemical production, use, and waste disposal (Wang et al., 2020). Under chronic exposure, the levels of these chemicals in bodily fluids, such as blood and urine, are likely to be correlated to the levels at the site of target organs and hormone receptors, which govern the possibility and severity of health impacts. For this reason, it is vital to understand the dosimetric relationship between the human intake dose of a chemical (an “external dose”) and its resulting concentrations within bodily fluids (related to an “internal dose”). For example, biomonitoring studies measure chemical levels present in the human body, whereas toxicological benchmarks derived from *in vivo* animal studies and adjusted for various uncertainty factors, such as interspecies extrapolation, are often expressed as external doses representing safe levels of human exposure to chemicals. Examples of such toxicological benchmarks include the reference dose recommended by the U.S. Environmental Protection Agency and the minimal risk level used by the U.S. Agency for Toxic Substances and Disease Registry. In such a case, quantitative knowledge of the dosimetric relationship enables converting toxicological benchmarks to corresponding concentrations in the human body, often termed “biomonitoring equivalents” (BEs), bridging the gap between toxicological and biomonitoring data to inform health risks (Tan et al., 2007; Wambaugh et al., 2013). Additionally, such a dosimetric relationship can be used in reverse dosimetry to back calculate the initial dose of a compound that supports generating chemical concentrations in blood and urine, notably concentrations that can produce adverse bioactivity (Judson et al., 2011; Mage et al., 2004; Rotroff et al., 2010; Tan et al., 2007; Wambaugh et al., 2013, 2014). A

prominent example is the U.S. Environmental Protection Agency's ExpoCast program, wherein urinary concentrations of chemical metabolites reported in the National Health and Nutrition Examination Survey (NHANES) biomonitoring program were used to predict the average daily intake doses of their original parent compounds (Wambaugh et al., 2014). In addition, the dosimetric relationship allows converting route-specific (such as ingestion or inhalation) toxicological potency (e.g., the threshold of toxicological concern) into blood concentrations (J. Arnot et al., 2022; Ellison et al., 2019; Partosch et al., 2015). With a widely accepted notion that doses from different routes are equivalent if they yield the same blood concentration, this conversion renders doses from different exposure routes comparable and extrapolatable (Partosch et al., 2015; Pepelko & Withey, 1985). This lays a quantitative basis for route-to-route extrapolation between route-specific toxicological benchmark doses (Partosch et al., 2015; Pepelko & Withey, 1985).

When assessing the dosimetric relationship, it is important to consider the chemical properties of different compounds, including partition coefficients that describe a chemical's hydrophobicity and volatility as well as biotransformation half-lives that describe a chemical's resistance to metabolism in the human body. These properties are important because they affect how each compound interacts with internal absorption barriers and different mechanisms of elimination. Earlier studies on cows (Birak et al., 2001; Dowdy et al., 1996; Research Triangle Institute, 2005; Travis & Arms, 1988) have elucidated the dependence of the dosimetric relationship, characterized by a "biotransfer factor" defined as the ratio of chemical concentration in beef or milk to intake dose through feeding, on octanol-water partition coefficient (K_{ow}) that quantifies hydrophobicity (Birak et al., 2001; Dowdy et al., 1996; Research Triangle Institute, 2005;

Travis & Arms, 1988). These studies showed that the biotransfer factors in beef and milk peaked at around a log K_{OW} of 6, owing to the efficient elimination of highly hydrophilic chemicals and minimal absorption of highly hydrophobic chemicals. That being said, those studies considered only partitioning properties and ignored biotransformation and other toxicokinetic processes. As such, their results apply only to those chemicals that undergo negligible biotransformation, such as persistent organic pollutants, and hence have limited applicability to chemicals with diverse biotransformation capabilities.

The contribution of fundamental chemical properties to the dosimetric relationship and the possible impacts of physiological factors (often age- and body weight-dependent) are still unclear. Since these chemical properties can often be obtained through laboratory testing or computational theory at an economical cost, revealing their quantitative connection to the dosimetric relationship enables us to forecast the bioaccumulative tendencies of different compounds. This helps in screening and prioritizing the vast number of chemicals on the market for their potential for human exposure and body accumulation. Earlier animal-based studies (Hendriks et al., 2007; Research Triangle Institute, 2005) used empirical statistical approaches, such as linear regression, to account for the impacts of one individual variable at a time, leading to a lack of inclusion of combined effects of chemical properties and physiological factors. Essentially, this limitation can be addressed by mechanistic modeling, i.e., using physiologically based toxicokinetic models building on chemical and physiological processes, by considering interactions among multiple variables. In most recent studies, toxicokinetic models were adopted to calculate the dosimetric relationship individually for several chemicals (Liao et al., 2007; Louisse et al., 2017; Wetmore, 2015). A remarkable variability of at least

three orders of magnitude in the calculated dosimetric relationships in these discrete case studies warrants a mechanistic, systematic understanding of how chemical properties govern the dosimetric relationship (Rotroff et al., 2010).

The objective of this study is to mechanistically and systematically understand (i) the variability in the dosimetric relationship among chemicals with vastly diverse properties and (ii) the possible impacts of physiological factors on the variability among subpopulations with different physiological conditions (e.g., obese vs. lean individuals, children vs. adults). The following study quantifies the dosimetric relationship by calculating a ratio of the daily chemical intake dose to the concentration in the human blood or urine, based on outputs from a well-evaluated, mechanistic toxicokinetic model (L. Li, Arnot, et al., 2018, 2019; L. Li, Westgate, et al., 2018). Such a ratio can gain broad applications in exposure science, toxicology, and risk assessment, especially in the era of “new approach methods”, e.g., determining equivalent doses for biomonitoring data comparison, estimating route-to-route extrapolation values, and back calculating the steady-state daily intake dose of a chemical. We identify partition coefficients and biotransformation half-lives whereby chemicals can be found at high concentrations when the daily intake dose is equal. Partition coefficients and biotransformation half-lives are selected here due to their frequent use in environmental exposure science (Mackay et al., 2015) and the ability of prediction tools to reliably compute these values for most environmental chemicals (L. Li et al., 2022). Results are visualized in a series of chemical partitioning plots, from which the order of magnitude of a chemical’s dose-to-concentration ratio (DCR) can be quickly read based on its partition coefficients between air, water, and octanol phases. We also explore whether such property dependence is

similar for both adults and children and for individuals with normal body weights and with obesity.

The novelty of this work lies in that it reveals a series of general trends and principles describing the impacts of chemical properties on the route-specific dosimetric relationship. Complementing existing chemical-by-chemical estimates, e.g., those cited by Ref. (Rotroff et al., 2010), our work provides mechanistic insights into chemical properties that contribute to high accumulation in the human body. Such insights can inform the risk estimation and assessment of the vast number of chemicals and can be applied proactively even before the production or commercialization of chemicals. Therefore, our gained knowledge has the potential to support decision-making regarding the safe and responsible use of chemicals. Furthermore, the knowledge can also inform biomonitoring studies that typically measure overall chemical levels in the human body without distinguishing between multiple exposure routes and multiple elimination processes.

2. Methods:

2.1 Define the dose-to-concentration ratio (DCR):

Here, we quantified the dosimetric relationship using the ratio of daily intake dose (in $\mu\text{g}/\text{d}$) to chemical concentration in biological fluids (blood or urine; in $\mu\text{g}/\text{L}$), defined as DCR with a unit of L/d . It links the external dose with the internal occurrence of a chemical. Numerically, the DCR also represents the volume of blood or urine where contamination of a chemical can be contaminated over a unit of time. The DCR is assumed to be independent of the intake dose. This assumption is sound when metabolic

biotransformation follows the first-order reaction, which is often the case at the typical exposure levels anticipated for industrial and environmental chemicals (Wetmore, 2015).

We limit the scope of this work to the following. First, we focus on parent compounds only and do not include corresponding metabolites. That is, we consider the removal of parent compounds from the body as a route of elimination, rather than considering the generation of bioactive metabolites. We also assume that exposure to chemicals and associated metabolites does not initiate irreversible effects that, in turn, adversely impact absorption and elimination processes. Second, we focus on DCRs at the steady state given that the steady state represents conservative estimates of reasonable worst situations in health risk and impact assessments (De Bruijn et al., 2002). Third, we use the “total” chemical concentrations in blood and urine, for example, combining both the freely dissolved and cell- or protein-bound chemicals in the blood. For detailed discussions on these assumptions, please see Section 4 “Implications and Limitations”.

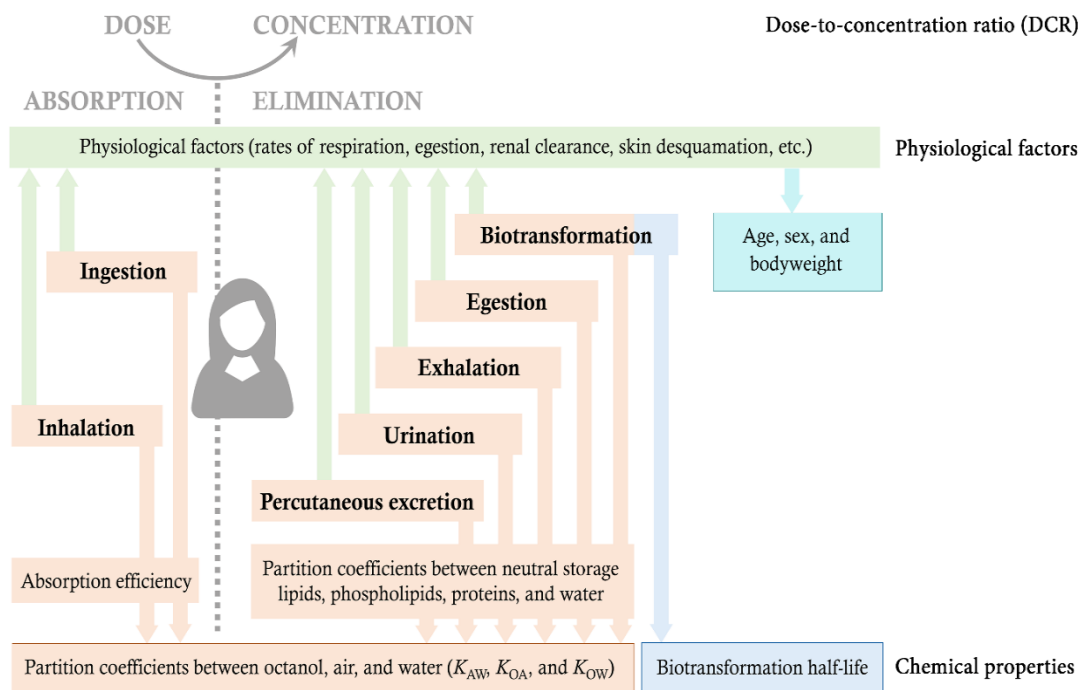


Figure 1. Schematic overview of PROTEX's human exposure and toxicokinetic module. It calculates chemical concentrations in blood and urine resulting from a single unit dose of chemical intake by mechanistically quantifying absorption and elimination processes as functions of chemical properties (partition coefficients between octanol, air, and water and biotransformation half-life) and physiological factors (such as functions of age, sex, and bodyweight). For illustration purposes, the model is parameterized to represent a 25 year old archetypal female American (Results for Sections 3.1 through 3.3). Additional computations are conducted for a 3 year old female child and an obese individual with a bodyweight and fat weight twice that of the American average (Results for Section 3.4).

2.2 Simulations of DCRs on the PROTEX model:

We simulated the dose-to-blood concentration (DCR_{blood}) and dose-to-urinary concentration (DCR_{urine}) using the human exposure and toxicokinetic module of a comprehensive chemical assessment model named PROduction-To-EXposure (PROTEX) (L. Li, Arnot, et al., 2018, 2019; L. Li, Westgate, et al., 2018). Figure 1 presents a schematic overview of the core structure of PROTEX's human exposure and toxicokinetic module and its dependence on chemical properties. Briefly, the module predicts the age-dependent level of chemicals in biological media (e.g., blood, urine, and

lipid) by mechanistically quantifying mass flows via multiple routes of absorption and elimination of chemicals by the human body (for details on route-specific considerations and quantification, see Appendix 1 and Appendix 2). To do so, the module considers the intestinal absorption of chemicals through ingestion of food and non-food items (e.g., dust, soil particles, and surface residuals), the respiratory absorption of chemicals through inhalation of air and airborne particles, as well as the dermal absorption of chemicals on the human skin (not discussed in this paper). For a given chemical, PROTEX predicts an “absorption efficiency”, i.e., the fraction passing the absorption barrier, based on its chemical properties (Kelly et al., 2004). On the other hand, it considers the elimination of chemicals through biotransformation and non-biotransformation processes (exhalation, egestion, urination, and percutaneous excretion). PROTEX quantifies elimination using a total elimination half-life (J. A. Arnot et al., 2014). The total elimination half-life should not be confused with the biotransformation half-life because the difference between these two half-lives reflects the excretion of chemicals through processes other than biotransformation. For women of childbearing age, PROTEX additionally characterizes the loss of chemicals through reproduction and lactation (L. Li, Arnot, et al., 2018), which are beyond the scope of this work. PROTEX characterizes the rates of chemical absorption and elimination as functions of age-, sex-, and bodyweight-dependent physiological factors (e.g., the rates of respiration, glomerular filtration, and skin desquamation) and chemical properties (partition coefficients and biotransformation half-lives). For detailed information, please see Refs. (L. Li, Arnot, et al., 2018; L. Li, Westgate, et al., 2018) Appendix 1 through Appendix 4 brief the calculation of chemical elimination processes, urinary concentrations of chemicals, and absorption efficiencies.

The parameterization of PROTEX requires input information on both the modeled individual and chemicals of interest. We parameterized the module to represent an archetypal female American whose anthropometric, physiological, and behavioral characteristics were representative of the medians (or averages if medians are not available) of U.S. females. A detailed description of this modeled individual can be found in Ref. (L. Li, Hoang, et al., 2019); the parameterization is consistent with up-to-date generic toxicokinetic models such as the generic physiologically based toxicokinetic (G-PBTK) model (Armitage et al., 2021) and the high-throughput toxicokinetic (HTTK) model (Pearce et al., 2017). The simulation was done for the entire lifetime of this modeled individual. In this paper, we discuss the results of age 25 in detail while presenting the results of age 3 as well. For comparison, we also ran PROTEX for obese individuals by doubling the default body weight and fat weight (following the assumption both groups have the same body fat percent) and hence changing the bodyweight-dependent physiological parameters in the model. That being said, this assumption may not hold true in all scenarios as previous studies have found variations between percent body fat for differing BMIs; however, the statistical significance of these variations has yet to be determined (Gallagher et al., 2000; Kyle et al., 2003).

PROTEX's expression of absorption and elimination processes requires inputs of a chemical's partition coefficients and biotransformation half-lives. For instance, PROTEX's algorithm utilizes partition coefficients between water, air, and biologically relevant phases, such as neutral lipids, phospholipids, and proteins. In this work, these partition coefficients are further quantified from partition coefficients between air and water (K_{AW}), between octanol and air (K_{OA}), and between octanol and water (K_{OW}), using

single-parameter linear free energy relationships (spLFERs) (Endo et al., 2011, 2012; L. Li et al., 2022). These three partition coefficients follow a thermodynamic triangular relationship ($\log K_{OW} = \log K_{OA} + \log K_{AW}$), allowing the calculation of each based on the other two. For each chemical, internal energies for adjusting the partition coefficients at 25 °C to their corresponding values at the human body temperature are calculated according to MacLeod et al. (MacLeod et al., 2007) PROTEX also requires input of the whole-body biotransformation half-life (HL_{human}) to characterize a chemical's tendency to resist metabolic biotransformation. PROTEX calculates the overall elimination half-life by considering biotransformation and non-biotransformation elimination processes.

2.3 Investigation into the impacts of chemical properties:

To investigate the impacts of chemical properties on DCRs, we repeatedly ran PROTEX to simulate blood and urinary concentrations (in $\mu\text{g/L}$) in response to a “unit” dose through ingestion or inhalation ($1 \mu\text{g/d}$), for a series of combinations of K_{AW} and K_{OA} ranging from 10^{-7} to 10^4 and from 10^2 to 10^{13} , respectively, with an infinite biotransformation half-life (i.e., “perfectly persistent”) and a biotransformation half-life of 2 days (close to the central tendency of more than 12,000 organics on chemical lists by the Organization for Economic Co-operation and Development) (J. A. Arnot et al., 2012). These combinations of partition coefficients cover the properties of a wide spectrum of environmental chemicals (L. Li, Arnot, et al., 2019). We calculated DCR_{blood} and DCR_{urine} by dividing the unit dose of intake by the modeled concentrations. In addition, we simulated the efficiencies of intestinal and respiratory absorption and the relative importance of different routes of elimination as functions of chemical partitioning properties.

2.4 Calculation of chemical properties for model performance evaluation:

To evaluate PROTEX's performance, we ran the model with partitioning and biotransformation properties of chemicals based on literature-reported measurements. Following the recommended best practices, (L. Li et al., 2022) the partition coefficients of the non-ionizable chemicals and the neutral form of ionizable chemicals were the consensus values of predictions by OPEN structure–activity/property Relationship App (OPERA), (Mansouri et al., 2018) poly parameter linear free energy relationships (pp-LFERs) (with Abraham solute descriptors computed by the Iterative Fragment Selection (IFS-QSAR)) (T. Brown, 2022), and EPI Suite (U.S. Environmental Protection Agency, 2012). The acid dissociation constants of ionizable chemicals were computed using OPERA and used to calculate distribution ratios at the body pH. The biotransformation half-lives were consensus values of predictions by IFS-QSAR and QSAR-INSubria-Chem (QSARINS-Chem). According to the IFS-QSAR and QSARINS-Chem training sets, (J. A. Arnot et al., 2014) these predictions represent the overall biotransformation half-lives, including biotransformation before (i.e., the first pass effect) (Varma et al., 2010) and after intestinal absorption.

3. Results and Discussion:

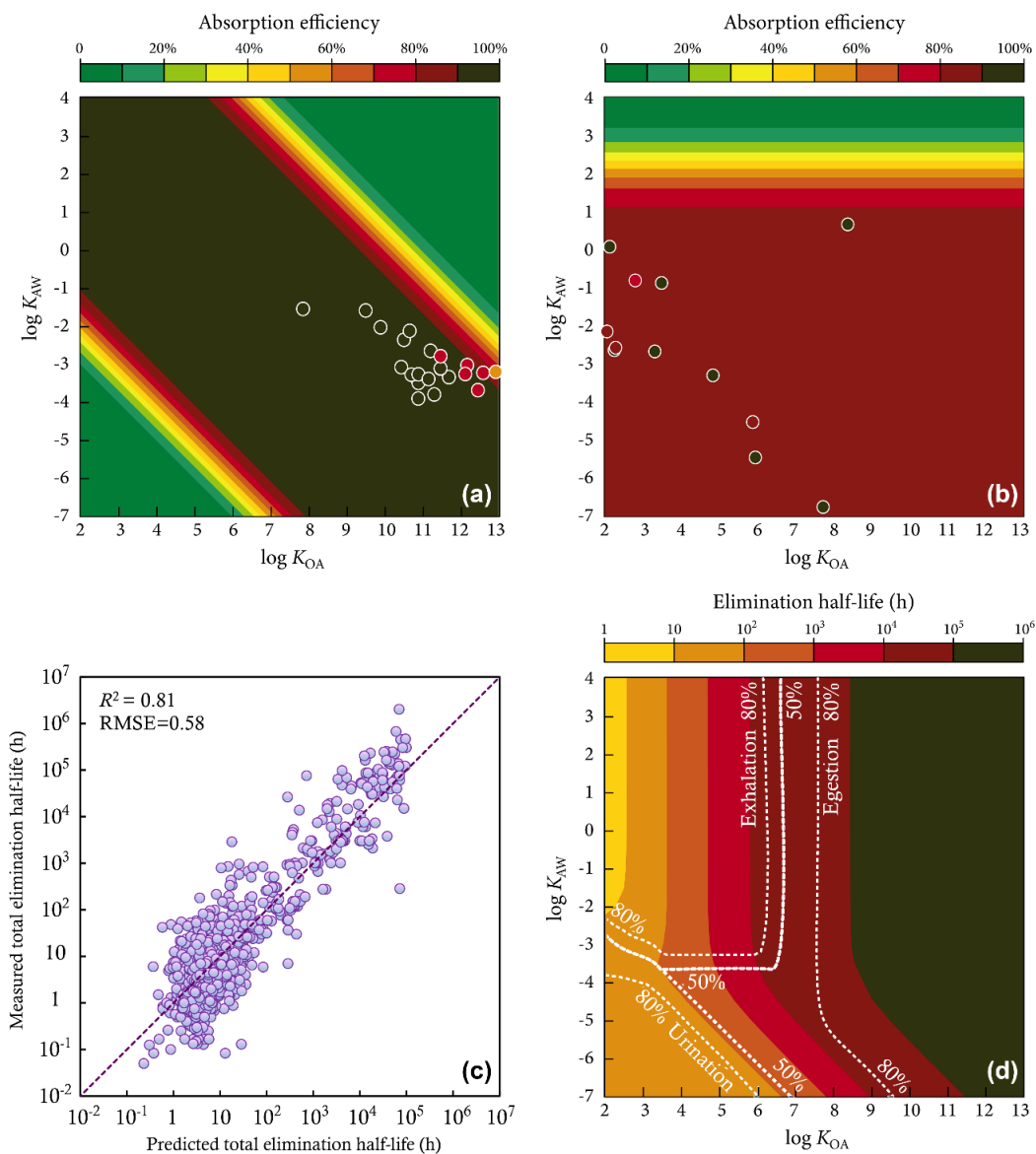


Figure 2. PROTEX-predicted efficiencies through intestinal (Panel a) and respiratory (Panel b) absorption (contour diagrams) as a function of $\log K_{AW}$ and $\log K_{OA}$ in comparison with literature-reported measurements (colored dots). Comparison between the modeled and literature-reported total elimination half-lives (Panel c). PROTEX-predicted half-lives for combined non-biotransformation elimination processes (exhalation, egestion, urination, and percutaneous excretion considered in this work) and the dominant processes of elimination (Panel d).

3.1 Evaluation of model performance:

Before interpreting and analyzing the relationship between chemical intake and concentrations, we first thoroughly evaluate PROTEX's performance in predicting human exposure and toxicokinetics to gain confidence in the model's fidelity. The evaluation is performed from two aspects: **First**, we evaluate the model's capability to capture the quantitative relationship between (i) toxicological benchmark doses and "biomonitoring equivalents" (BEs) for six chemicals with available data from the literature (Hays et al., 2007, 2008) and (ii) steady-state blood concentration normalized by 1 unit dose of exposure for 4 chemicals with available data in the literature (Aylward et al., 2010; Tan et al., 2007; Wambaugh et al., 2013). **Second**, since DCR depends on completing the absorption and elimination processes, we additionally evaluate the model's performance in predicting the intestinal and respiratory absorption efficiencies (41 chemicals collected from the literature) as well as the observed overall elimination half-lives (1,100 chemicals collected from the literature) (J. A. Arnot et al., 2014). Future studies may benefit from the model's encouraging performance of predicting the overall elimination half-life, which is critical for quantifying the connection between chemical intake and body concentrations but has been recognized as an "important scientific challenge" because oftentimes "current literature half-lives are not consistent" (Wong et al., 2013).

BEs are representative of the steady-state concentration of chemicals in a biological medium (mainly blood and urine) when an average human's chemical exposure equals a toxicological benchmark (e.g., a reference dose) (Hays et al., 2007, 2008). In this sense, our calculated DCR can be seen as the ratio of the toxicological benchmark to the

corresponding BE. Appendix 5 – Table A.1 compares our calculated DCRs with ratios derived from the toxicological benchmark doses and BEs, for ten environmental pollutants (Aylward et al., 2010; Aylward & Hays, 2008, 2011; Hays et al., 2012; Kirman et al., 2011; Krishnan et al., 2010, 2011). The results demonstrate that eight of the ten chemicals tested were within two orders of magnitude of each other with the predicted values being higher than the “real” measured values. This variation may be due to differing initial methods of deriving BE across the literature. For example, our predicted DCRs are closest to those measured using interspecies extrapolation (hexachlorobenzene, 2,4-D, and DDT) and PBTK modeling (benzene, bisphenol A, triclosan, and parathion), presumably due to increased accuracy within these methods. In contrast, our predicted DCRs differ most from BE values derived from the simple first-order elimination model (e.g. 2,2',4,4',5-PentaBDE), which may be a result of inaccurate assumptions made about variables such as absorption rate and half-life. For a more detailed discussion see Appendix 5 – Table A.1.

Figures 2a, b visualize the predicted absorption efficiencies for different combinations of $\log K_{OA}$ and $\log K_{AW}$, representing various possible chemicals in the partitioning space for intestinal and respiratory routes, respectively. Diagonals from the top left to the bottom right of these two-dimensional contour diagrams represent chemicals with the same $\log K_{OW}$. Real neutral chemicals can be placed on the diagrams based on their specific $\log K_{OA}$ and $\log K_{AW}$ values. Ionizable organic chemicals can be located by their distribution ratios $\log D_{OA}$ and $\log D_{AW}$, namely the abundance-weighted averages of the partition coefficients of their neutral and charged forms at the body pH. PROTEX predicts that intestinal absorption efficiencies are the highest for chemicals

with a log K_{OW} between 1 and 9 (Figure 2a), whereas respiratory absorption is most efficient for water-soluble chemicals with a log K_{AW} lower than 1 (Figure 2b). Figures 2a, b show that these predicted trends were generally confirmed by the medians of measurements for human intestinal (23 chemicals) (Andreas Moser & McLachlan, 2001) and respiratory (18 chemicals) (Baker & Dixon, 2006; Kuga et al., 2020) absorption efficiencies. Within these studies, for intestinal absorption efficiency, net absorption was reported as the amount of a chemical absorbed proportionate to its measured daily intake. This was reported as a percentage comparable to our model predicted absorption efficiency values. To measure the absorption rate in these studies, blood and fecal matter were collected and analyzed for concentrations of a given chemical (Andreas Moser & McLachlan, 2001). For respiratory absorption there were many factors taken into consideration when measuring the absorption efficiency which consist of a chemical's partition coefficients, level of initial smoke contamination, settled aerosol particles and resulting vapor phase contaminants from such particles. Within the studies there were two main methods used to measure the absorption efficiency of a given chemical involving the measurement of quantities within venous plasma and utilizing measured respiratory retention rates. Both of these methods report the amount of chemical intake relative to the dose value resulting in an absorption efficiency percentage (Baker & Dixon, 2006; Kuga et al., 2020). It is important to note that by using venous plasma as an absorption efficiency measurement the resulting values may be increased due to chemical absorption via the oral cavity during the smoking process. When comparing the measured values to our model predicted values this may be one reason for slight discrepancies between the two absorption efficiencies, however the values vary only slightly and

therefore still help to validate the reliability of our predicted values. These predicted trends are also consistent with literature-reported findings for other mammals. For instance, intestinal absorption has been shown to be rather limited for super hydrophilic ($\log K_{OW}$ below -0.5) or hydrophobic chemicals ($\log K_{OW}$ above 7) (O'Connor et al., 2013). The penetration of these chemicals is hindered by the lining of the intestinal tract, which combines hydrophilic (the unstirred water layer and epithelium) and hydrophobic (the epithelium) membranes (Zhang et al., 2021). For inhalation, however, less water-soluble chemicals, those with a $\log K_{AW}$ greater than -1, are less likely to be absorbed because the water-rich mucous resists their penetration through the respiratory epithelia (Zhang et al., 2021). Nevertheless, measurements are currently limited and often divergent from each other. For instance, PROTEX predicts a respiratory absorption efficiency of 86% for nicotine; however, the measurements vary from nearly 70% to almost 100% depending on the respiratory pattern and the composition of the inhaled mixtures (Baker & Dixon, 2006; Kuga et al., 2020).

Lastly, we use PROTEX's human toxicokinetic module to simulate the total elimination half-lives of 1,100 chemicals and compare the predictions with measurements collected by Arnot et al. (Figure 2c) from various accredited sources within the literature (J. A. Arnot et al., 2014). This collection process was done by searching through pharmacokinetic and toxicokinetic sources containing measured half-lives for organic chemicals in human adults. These 1,100 chemicals are diverse in physicochemical properties, ranging from hydrophobic to hydrophilic ($\log K_{OW}$ from 5 to 11), volatile to minimally volatile ($\log K_{OA}$ from 2 to 13), and recalcitrant to labile (HL_{human} from 1 to 10^6 h). Figure 2c indicates that the predicted and measured total elimination half-lives

show a strong correlation. The root-mean-square deviation (RMSE) between the predicted and measured total half-lives is 0.58 log units, indicating that the model overall succeeds in predicting the elimination processes for a wide range of chemicals with a discrepancy within an order of magnitude. The PROTEX's algorithm explains 81% of the variation ($R^2=0.81$). Appendix 6 – Figure A.1 indicates the residual (namely the difference between predicted and measured half-lives) seems to be random, independent of chemical partitioning (K_{OA} and K_{AW}) and biotransformation (HL_{human}) properties. With there being no evident pattern to the outlying chemicals, we anticipate no systematic bias present within the half-life predictions. Additionally, we identify 93 outliers, for which the predicted and observed half-lives diverge by over an order of magnitude. This discrepancy can be attributed to varying levels of uncertainty and possible error in measurements. For instance, our predicted total elimination half-life of PCB-156 (2 years) was 13 times shorter than the measurement documented in the dataset (26 years) (J. A. Arnot et al., 2014). Such a discrepancy is smaller than the variability in PCB-156 total elimination half-lives observed among several biomonitoring studies for adults, ranging from 1.6 to >100 years (Milbrath et al., 2009). According to Shirai and Kissel, (Shirai & Kissel, 1996) half-lives either shorter than 1 year or longer than 10 years may be very unlikely for PCBs. Also, when measurements are taken, they may not necessarily represent the steady-state level of a chemical (J. A. Arnot et al., 2014). This discrepancy is due to the difficulty in telling if steady-state was reached at the time of the collection of the data.

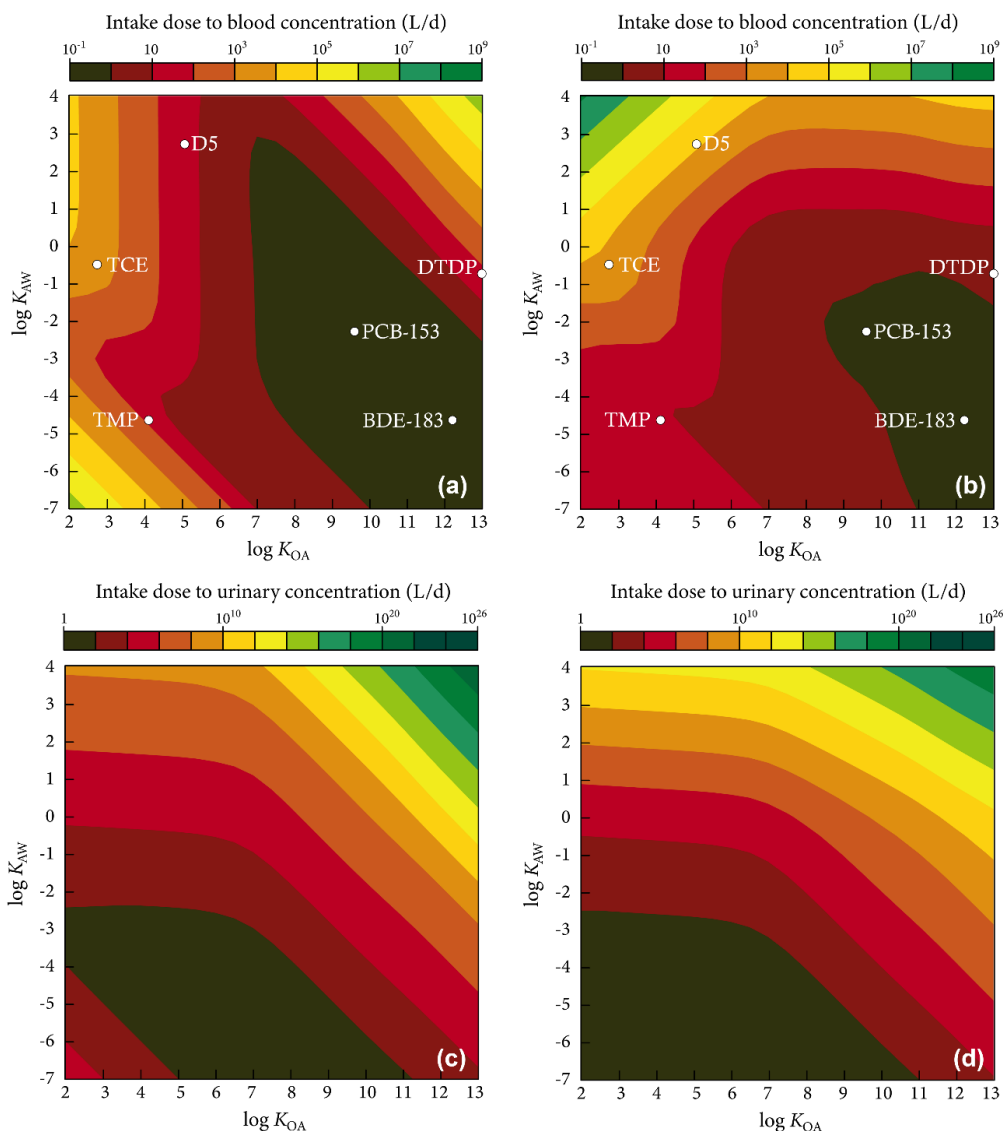


Figure 3. Chemical partitioning space illustrating the ratio of intake dose to blood concentration (DCR_{blood}) for ingestion (Panel a) and inhalation (Panel b) as well as the ratio of intake dose to urinary concentration (DCR_{urine}) for ingestion (Panel c) and inhalation (Panel d) of **hypothetical perfectly persistent chemicals** (molar mass = 300 g/mol) by an archetypal 25 year old female American. Chemicals are arranged by $\log K_{\text{AW}}$ and $\log K_{\text{OA}}$; diagonals represent chemicals with equal $\log K_{\text{OW}}$. Illustrative chemicals are marked based on their $\log K_{\text{AW}}$ and $\log K_{\text{OA}}$: PCB = polychlorinated biphenyl; PBDE = polybrominated diphenyl ether, D5 = decamethylcyclopentasiloxane (cyclic volatile methyl siloxane), DTDP = ditridecyl phthalate, TCE = trichloroethylene, and TMP = tris(methyl) phosphate.

3.2 Occurrence of perfectly persistent organic chemicals in the blood

After gaining confidence in the model's performance, we begin our discussion with

the simplest case of perfectly persistent chemicals, namely, recalcitrant chemicals not subject to metabolic biotransformation. Figure 3 visualizes the simulated DCR_{blood} for different combinations of $\log K_{OA}$ and $\log K_{AW}$, representing various possible hypothetical perfectly persistent chemicals as results of exposure through ingestion (Figure 3a) and inhalation (Figure 3b). Overall, the DCR_{blood} varies by more than 10 orders of magnitude among chemicals. In other words, we can expect the blood concentrations of various chemicals to differ by 10 orders of magnitude even if their intake doses are similar. This range is not unexpected because of the range (11 orders of magnitude for partition coefficients, as shown in Figure 3) of vastly diverse properties being analyzed for various chemicals and the effects these properties have on their absorption and elimination rates. Note that a lower DCR_{blood} (e.g., dark red areas in Figures 3a, b) means a higher blood concentration, with the intake dose being equal. Interestingly, the U.S. Environmental Protection Agency's ExpoCast project predicted that for general Americans, the average population median intake rate varies by 8 orders of magnitude among ~480,000 chemicals (Ring et al., 2019). Combining the variabilities in DCR_{blood} , we would expect chemical concentrations to vary by up to 18 orders of magnitude in Americans.

For both ingestion and inhalation, persistent chemicals with a high $\log K_{OA}$ and low $\log K_{AW}$ (lowly volatile and moderately to highly hydrophilic chemicals on the bottom right) were predicted to have the highest chemical concentration in blood if possessing the same intake doses as other chemicals. When this is paired with the dependence of absorption efficiencies for ingestion (Figure 2a) and inhalation (Figure 2b) on partitioning properties, these identified chemicals are within the range of highest

absorption efficiency. Furthermore, when ingestion and inhalation are directly compared, ingestion leads to higher DCR_{blood} at lower $\log K_{\text{OA}}$ and higher $\log K_{\text{AW}}$ (highly volatile but lowly hydrophilic chemicals on the upper left corner) than inhalation does because these chemicals are subject to efficient intestinal absorption (Figure 2a) but less efficient at diffusing through alveolar mucus, although they can freely move within the human airway (Zhang et al., 2021).

However, a high absorption efficiency does not necessarily lead to a high concentration in blood if the chemical is readily eliminated from the human body. For facilitating the interpretation, Figure 2d displays the dependence of the total non-biotransformation elimination half-life (in hours; resulting from combined routes of elimination other than biotransformation) on partitioning properties, as well as the PROTEX-predicted dominant routes of elimination (exhalation, urination, fecal egestion, and percutaneous excretion). Figures 3a, b show that chemicals with a small $\log K_{\text{OA}}$ (highly volatile chemicals on the left) and small $\log K_{\text{OW}}$ (highly hydrophilic chemicals in the bottom left corner) have high DCR_{blood} . This is mostly because these chemicals are efficiently eliminated from the human body through exhalation, urination, or percutaneous excretion, respectively (Figure 2d). In contrast, chemicals with the lowest DCR_{blood} are those with the longest elimination half-life (Figure 2d). Since these chemicals are less volatile (with a high $\log K_{\text{OA}}$) and less water-soluble (with a high $\log K_{\text{OW}}$), elimination through exhalation, urination, and percutaneous excretion is rather slow. Given that fecal egestion is usually not an efficient route of elimination, these chemicals may stay in the human body for a long time before reaching a heightened level.

Taken together, Figures 3a, b underscore that DCR_{blood} reflects a competition between the absorption and elimination processes. Figures 3a, b display four main mechanisms that lead to different DCR_{blood} : (I) high absorption and low elimination (chemicals on the bottom right), with typical examples including polychlorinated biphenyls and polybrominated diphenyl ethers, (II) high absorption and high elimination (chemicals on the upper left for ingestion and chemicals on the bottom left for inhalation), with typical examples including cyclic volatile methyl siloxanes, (III) low absorption and low elimination (chemicals on the upper right), with typical examples including dinitridecyl phthalate, and (IV) low absorption and high elimination (chemicals on the bottom left for ingestion and chemicals on the upper left for inhalation), with typical examples including organic solvents such as trichloroethylene, and water-soluble organophosphates such as tris(methyl) phosphate.

We also predicted the DCR_{urine} for different combinations of $\log K_{\text{OA}}$ and $\log K_{\text{AW}}$, representing hypothetical perfectly persistent chemicals (Figure 3c, d). For both ingestion (Figure 3c) and inhalation (Figure 3d), chemicals with a low $\log K_{\text{AW}}$ and a low $\log K_{\text{OW}}$ (highly hydrophilic chemicals on the bottom left) share the lowest DCR_{urine} . In other words, compared to other chemicals, these chemicals can be found more abundant in the urine even if sharing the same levels of intake dose. Recalling Figure 2d, we can find that chemicals within this range tend to be fairly water-soluble, so inevitably, they would be eliminated through urination.

Interestingly, Figure 3 reveals that DCR_{blood} is governed by both absorption and elimination, whereas DCR_{urine} is to a greater extent governed by elimination. In other

words, chemicals that tend to be eliminated through urination are more likely to achieve a high urinary level, with the intake dose remaining equal. Nevertheless, for the ingestion route, the less efficient intestinal absorption still limits the DCR_{urine} of chemicals with $\log K_{ow}$ lower than -2, as evidenced by the bottom left side corner of Figure 3c.

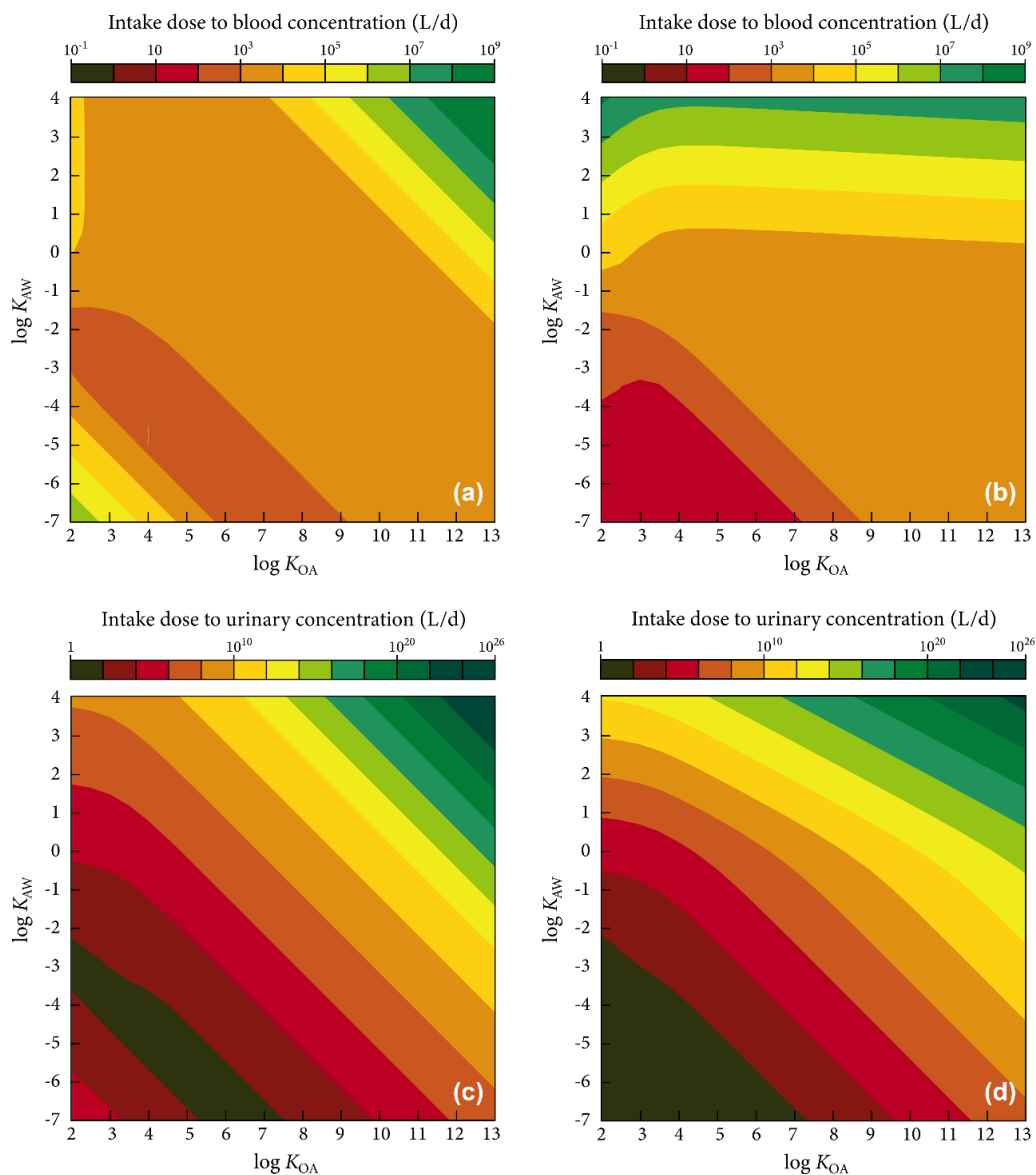


Figure 4. Chemical partitioning space illustrating the ratio of intake dose to blood concentration (DCR_{blood}) for ingestion (Panel a) and inhalation (Panel b), as well as the ratio of intake dose to urinary concentration (DCR_{urine}) for ingestion (Panel c) and inhalation (Panel d), of chemicals (molar mass = 300 g/mol) with a **human whole-body biotransformation half-life of 2 days**, by an archetypal 25-year-old female American. Chemicals are arranged by $\log K_{AW}$ and $\log K_{OA}$; diagonals represent chemicals with equal $\log K_{ow}$.

3.3 Occurrence of labile organic chemicals in blood and urine

We additionally consider how the biotransformation of a chemical impacts the DCR, given that organic chemicals can be subject to different extents of hepatic and intestinal biotransformation (J. A. Arnot et al., 2014). As compared to the perfectly persistent chemicals shown in Figure 3, chemicals possessing the same partitioning properties but undergoing rapid biotransformation (with a whole-body biotransformation half-life of 2 days), are selected in Figure 4 as an illustrative example. Note that the PROTEX model can also be parameterized to represent more persistent or labile chemicals if desired.

Overall, compared with perfectly persistent chemicals, chemicals that undergo negligible biotransformation have increased DCRs. Such an increase is more pronounced for perfectly persistent chemicals already with low DCRs, namely chemicals with a high $\log K_{OA}$ and low $\log K_{AW}$ (chemicals on the bottom right) for DCR_{blood} and chemicals with a low $\log K_{AW}$ and a low $\log K_{OW}$ (chemicals on the bottom left) for DCR_{urine} . Notably, for chemicals with a $\log K_{OW}$ between 4 and 10 and a $\log K_{OA}$ greater than 7, DCR_{blood} increased by 3 orders of magnitude from the case of perfect persistence (Figure 3a) to that with a biotransformation half-life of 2 days (Figure 4a), regardless of exposure routes. This is because these chemicals are associated with long non-biotransformation elimination half-lives (corresponding to elimination processes other than biotransformation, including exhalation, egestion, urination, and percutaneous excretion considered in this work; see Section 2.2), typically longer than 10,000 h (Figure 2d); therefore, the inclusion of a fairly short biotransformation half-life of 2 days substantially lowers the overall elimination half-life and greatly reduces the chemical level in the

human body. In contrast, since the non-biotransformation elimination half-lives are already short for volatile, hydrophilic chemicals (less than 1,000 h; Figure 2d), the inclusion of a biotransformation half-life of 2 days only slightly alters the total elimination half-life and poses minimal impacts on DCRs.

3.4 Impacts of physiological factors on the dose-to-concentration ratio

In previous sections, we based our modeling on an archetypal female American aged 25. One may wonder whether, and to what extent, the above results hold for individuals other than a 25-year-old archetypal adult, such as children, obese individuals, and other vulnerable subpopulations in environmental health. Underlying this is the question of whether physiological factors have a more significant impact on the DCR than chemical properties.

Since the mechanistic nature of the PROTEX model enables exploring the interaction of chemical properties and physiological factors, we additionally calculated DCR_{blood} and DCR_{urine} of the hypothetical perfectly persistent chemicals for a child three years of age (Appendix 7 – Figure A.2) and an adult with a higher than average body weight (Appendix 8 – Figure A.3), through ingestion and inhalation. In comparison with those found earlier for an archetypal 25-year-old American woman (Figures 3 & 4), despite a difference in the levels of DCR_{blood} and DCR_{urine} , the resulting distribution of hot spot areas in the outcomes of each simulation was similar. Notably, the DCR_{blood} is almost unchanged for chemicals with a $\log K_{\text{OA}}$ lower than 6.5 or chemicals with a $\log K_{\text{OW}}$ lower than 3. These chemicals are readily eliminated via exhalation and urination, respectively, and their distribution is less dependent on physiological parameters.

The differences seen between children and adults are due to the children's more efficient elimination of chemicals from their bodies (Ginsberg et al., 2004). This has been observed in extensive biomonitoring studies (Kerger et al., 2006; Milbrath et al., 2009). PROTEX predicts that the non-biotransformation elimination half-life of a given chemical is 1.8 to 5.5 times longer in adults than in children. Such a discrepancy is more pronounced for chemicals that are eliminated mainly through fecal egestion because children eat and defecate more relative to their body weight than adults do. For this reason, the DCR_{blood} of these chemicals are more responsive to age (Appendix 7 – Figure A.2). It should be noted that PROTEX here calculates the “true” non-biotransformation elimination half-life, which excludes the dilution effect of the fast growth of children; the adult-child difference in the “apparent” non-biotransformation elimination half-life would become more remarkable should this effect be considered (Clewell et al., 2004).

Furthermore, for those whose body weight is above average (Appendix 8 – Figure A.3), the outcome was comparable to those of average weight. The increased fat volume found in an overweight adult increases the storage of hydrophobic chemicals and reduces entry into systemic circulation leading to their possible elimination (La Merrill et al., 2013; L. Li & Wania, 2017). Therefore, though overweight adults would in fact have higher burdens (total masses) of hydrophobic chemicals found within their entire body, the levels of these chemicals found specifically in their blood are similar to the levels of hydrophobic chemicals found within the blood of an average adult, leading to similar outcomes within the DCR. It is important to recognize that given the PROTEX model utilizes a generic total lipid fraction in whole blood regardless of an individual's body composition status (average or obese), and therefore expected increase in cholesterol

levels within the blood for an obese individual has not been taken into consideration. Based on previous studies cholesterol levels between differing BMIs have shown statistical significance or strong correlations between increased cholesterol levels and comparison between average and obese populations (Hertelyova et al., 2016; Szczygielska et al., 2003). Therefore, taking into consideration increased cholesterol for obese populations in future studies would help to increase the accuracy of our predicted values.

These similarities between the modeled scenarios go to show that both age- and weight-dependent physiological variabilities play a limited role in governing a chemical's DCR_{blood} and DCR_{urine} . That being said, if a hypothetical perfectly persistent chemical falls along the outside region of changing zones, there may be some numeric differences. While it is important to note this, the differences are small enough to still have comparable results among the modeled scenarios.

Based on these findings, it is believed that the conclusions in this work are generic and may also be applied to people from other countries and yield similar results. For obtaining more accurate population- and region-specific results, one can also run the PROTEX model, as long as the needed information about the population being observed is entered into the PROTEX model. If there are specific chemicals of interest, then the properties of these chemicals may also need to be entered. As shown in the simulations above, chemicals that undergo both substantial and negligible biotransformation within a population can be analyzed via this method.

4 Implications and Limitations:

This work offers a pioneering systematic understanding of the quantitative relationship between the human intake dose and concentrations in bodily fluids for chemicals, taking into account the diversity of chemical partitioning and biotransformation properties. It discloses the dependence of the calculated DCR on the interaction between chemical properties and the physiological properties. This systematic understanding is especially useful in the “new approach methods” era because it enables a rapid preliminary evaluation of a chemical’s accumulation potential using only its readily available properties and general rules and principles outlined in this study, saving both time and resources. It also allows for the comparability between chemicals to identify the concerning properties based on which production can be regulated. Such information parsimony allows for high-throughput exposure assessments for numerous chemicals already on the market, as well as for the data-poor premanufactured and designed chemicals. Our chemical partitioning plots also facilitate quickly estimating the order of magnitude of the DCR_{blood} and DCR_{urine} for large numbers of chemicals based on only the information on partition coefficients and biotransformation half-lives. The PROTEX model itself can still provide more precise estimates of DCRs. Both can promote the applications of the DCR concept in exposure science, toxicology, and risk assessment. In environmental and health risk assessments, DCR can help convert estimated daily intake doses to concentrations in biological specimens, facilitating the use of biomonitoring data, e.g., biomarker concentrations measured in the U.S. NHANES and Canadian Health Measures Survey. For example, DCR can be used to derive BEs for comparisons with biomonitoring data to inform the risks posed to the general population

(Aylward et al., 2010; Aylward & Hays, 2008, 2011; Hays et al., 2012; Kirman et al., 2011; Krishnan et al., 2010, 2011).

DCR can also be used to calculate route-to-route extrapolation factors between benchmark doses derived following ingestion or inhalation exposures (Partosch et al., 2015; Pepelko & Withey, 1985). The extrapolation factors should be chemical specific because they reflect the combined effects of route-specific absorption and elimination. However, the absence of chemical specific factors results in the use of conservative estimates, for example, the assumed 50% for intestinal absorption and 100% for respiratory absorption recommended by the European Guidance on Information Requirements and Chemical Safety Assessment (European Chemical Agency, 2012). Noticing that the ratio of intestinal to respiratory absorption efficiencies is mathematically equivalent to the ratios between DCR_{blood} for ingestion and inhalation routes, we thus recommend using PROTEX-predicted DCRs based on chemical-specific data for more reasonable estimates in route-to-route extrapolation.

DCR also aids in screening-level reverse dosimetry to back calculate the steady-state daily intake dose that is not likely to cause observable adverse biological impacts based on *in vitro* bioactivity tests or other new approach methods (Judson et al., 2011; Rotroff et al., 2010; Wambaugh et al., 2015). Sharing a similar meaning with the commonly used guidance or reference toxicological benchmark doses, such back-calculated intake doses complement and expand existing databases of toxicological points of departure (Fantke et al., 2021). It also enables investigating the consistency between the toxicity characterized by *in vivo* toxicological data and *in vitro* bioactivity data (D. Li et al., 2020; Paul

Friedman et al., 2020).

DCR_{urine} can also be used to predict the occurrence of pharmaceuticals in urine and, hence, the urinary excretion of unmetabolized pharmaceuticals. Such information helps determine the environmental releases of pharmaceuticals for ecological risk assessments, which aims to promote sustainable pharmacy by decreasing pharmaceutical waste and safeguarding the ecological integrity (Orive et al., 2022).

Despite the wide implications of DCRs and mechanistic insights gained from this study, we must acknowledge the limitations of this work. First, we investigated the steady-state DCR because it represents the case of long-term, quasi-constant exposure to environmental chemicals. Although such a conservative scenario is desired for risk assessment, (De Bruijn et al., 2002) it is important to note this ratio may not be reflective of true chemical levels if chemicals have a long residence time within the human body, or if chemicals whose production and emissions are subject to substantial temporal changes. Second, the current work builds largely on the mechanistic understanding of neutral organic chemicals. While PROTEX's algorithm accommodates ionizable organic chemicals and performs satisfactorily for both neutral and ionizable organic chemicals, we should note that the mechanistic knowledge and quantitative characterization of the toxicokinetics of ionizable organic chemicals, e.g., the electrostatic interactions between charged chemicals and the body tissues, are still rather inadequate. Third, the current work focuses on the ingested and inhaled parent compounds and excludes their metabolites from the discussion. Compared to parent compounds, metabolites are typically more hydrophilic, hence, occupying different locations in the chemical

partitioning space (typically moving downward in the diagrams) (Cassarett & Doull, 1975). Also, the use of the DCR approach limited to the parent compound when working with more bioactive metabolites would not lead to the intended protective human health estimates. Fourth, in future work, dermal absorption should also be considered when assessing the DCRs for chemicals often found in consumer products, such as lotions, sunscreens, and make-ups.

References

- Andreas Moser, G., & McLachlan, M. S. (2001). The influence of dietary concentration on the absorption and excretion of persistent lipophilic organic pollutants in the human intestinal tract. *Chemosphere*, *45*(2), 201–211. [https://doi.org/10.1016/S0045-6535\(00\)00551-8](https://doi.org/10.1016/S0045-6535(00)00551-8)
- Armitage, J. M., Hughes, L., Sangion, A., & Arnot, J. A. (2021). Development and intercomparison of single and multicompartiment physiologically-based toxicokinetic models: Implications for model selection and tiered modeling frameworks. *Environ Int*, *154*, 106557. <https://doi.org/10.1016/j.envint.2021.106557>
- Arnot, J. A., Brown, T. N., & Wania, F. (2014). Estimating screening-level organic chemical half-lives in humans. *Environ Sci Technol*, *48*(1), 723–730. <https://doi.org/10.1021/es4029414>
- Arnot, J. A., Brown, T. N., Wania, F., Breivik, K., & McLachlan, M. S. (2012). Prioritizing chemicals and data requirements for screening-level exposure and risk assessment. *Environ Health Perspect*, *120*(11). <https://doi.org/10.1289/ehp.1205355>
- Arnot, J., Toose, L., Armitage, J., Sangion, A., Looky, A., Brown, T., Li, L., & Becker, R. (2022). Developing an internal threshold of toxicological concern (iTTC). *J Expo Sci Environ Epidemiol*, 877–884.
- Aylward, L. L., & Hays, S. M. (2008). Biomonitoring Equivalents (BE) dossier for 2,4-dichlorophenoxyacetic acid (2,4-D) (CAS No. 94-75-7). *Regul Toxicol Pharmacol*, *51*(3 SUPPL.), S37–S48. <https://doi.org/10.1016/j.yrtph.2008.05.006>
- Aylward, L. L., & Hays, S. M. (2011). Biomonitoring-based risk assessment for hexabromocyclododecane (HBCD). In *Int J Hyg Environ Health* (Vol. 214, Issue 3, pp. 179–187). <https://doi.org/10.1016/j.ijheh.2011.02.002>
- Aylward, L. L., Hays, S. M., Gagné, M., Nong, A., & Krishnan, K. (2010). Biomonitoring equivalents for hexachlorobenzene. *Regul Toxicol Pharmacol*, *58*(1), 25–32. <https://doi.org/10.1016/j.yrtph.2010.06.003>
- Baker, R. R., & Dixon, M. (2006). The retention of tobacco smoke constituents in the human respiratory tract. In *Inhal Toxicol* (Vol. 18, Issue 4, pp. 255–294). <https://doi.org/10.1080/08958370500444163>
- Birak, P., Yurk, J., Adeshina, F., Lorber, M., Pollard, K., Choudhury, H., & Kroner, S. (2001). Travis and Arms revisited: A second look at a widely used bioconcentration algorithm. *Toxicology and Industrial Health*, *17*(10), 163–175. <https://doi.org/10.1191/0748233701th110oa>
- Brown, E. A., Shelley, M. L., & Fisher, J. W. (1998). A pharmacokinetic study of occupational and environmental benzene exposure with regard to gender. *Risk Anal*, *18*(2), 205–213. <https://doi.org/10.1111/j.1539-6924.1998.tb00932.x>
- Brown, T. (2022). QSPRs for Predicting Equilibrium Partitioning in Solvent–Air Systems from the Chemical Structures of Solutes and Solvents. *Journal of Solution Chemistry*, *51*, 1101–1132.
- Cassarett, L. J., & Doull, J. (1975). Toxicology: the basic science of poisons. In *MACMILLAN PUBL., N.Y.* (Vol. 33, pp. 282–283). <https://doi.org/10.1136/oem.33.4.282-b>
- Clewell, H. J., Gentry, P. R., Covington, T. R., Sarangapani, R., & Teegarden, J. G. (2004). Evaluation of the potential impact of age- and gender-specific pharmacokinetic differences on tissue dosimetry. *Toxicol Sci*, *79*(2), 381–393. <https://doi.org/10.1093/toxsci/kfh109>
- Clewell, H. J., Gentry, P. R., Gearhart, J. M., Covington, T. R., Banton, M. I., & Andersen, M. E. (2001). Development of a physiologically based pharmacokinetic model of isopropanol and its metabolite acetone. *Toxicol Sci*, *63*(2), 160–172. <https://doi.org/10.1093/toxsci/63.2.160>
- De Bruijn, J., Hansen, B., Johansson, S., Luotamo, M., Munn, S., Musset, C., Olsen, S., Olsson, H., Paya-Perez, A., Pedersen, F., Rasmussen, K., & Sokull-Kluttgen, B. (2002). Technical

- Guidance Document on risk Assessment. *European Commission Joint Research Centre*.
Dowdy, D. L., Mckone, T. E., & Hsieh, D. P. H. (1996). Prediction of chemical biotransfer of organic chemicals from cattle diet into beef and milk using the molecular connectivity index. *Environ Sci Technol*, *30*(3), 984–989. <https://doi.org/10.1021/es950398c>
- Ellison, C. A., Blackburn, K. L., Carmichael, P. L., Clewell, H. J., Cronin, M. T. D., Desprez, B., Escher, S. E., Ferguson, S. S., Grégoire, S., Hewitt, N. J., Hollnagel, H. M., Klaric, M., Patel, A., Salhi, S., Schepky, A., Schmitt, B. G., Wambaugh, J. F., & Worth, A. (2019). Challenges in working towards an internal threshold of toxicological concern (iTTC) for use in the safety assessment of cosmetics: Discussions from the Cosmetics Europe iTTC Working Group workshop. *Regul Toxicol Pharmacol*, *103*, 63–72. <https://doi.org/10.1016/j.yrtph.2019.01.016>
- Endo, S., Bauerfeind, J., & Goss, K. U. (2012). Partitioning of neutral organic compounds to structural proteins. *Environ Sci Technol*, *46*(22), 12697–12703. <https://doi.org/10.1021/es303379y>
- Endo, S., Escher, B. I., & Goss, K. U. (2011). Capacities of membrane lipids to accumulate neutral organic chemicals. In *Environ Sci Technol* (Vol. 45, Issue 14, pp. 5912–5921). <https://doi.org/10.1021/es200855w>
- European Chemical Agency. (2012). *Guidance on information requirements and chemical safety assessment: Chapter R.8: Characterisation of dose (concentration)-response for human health*.
- Fantke, P., Chiu, W. A., Aylward, L., Judson, R., Huang, L., Jang, S., Gouin, T., Rhomberg, L., Aurisano, N., McKone, T., & Jolliet, O. (2021). Exposure and toxicity characterization of chemical emissions and chemicals in products: global recommendations and implementation in USEtox. *Int J Life Cycle Assess*, *26*(5), 899–915. <https://doi.org/10.1007/s11367-021-01889-y>
- Gallagher, D., Heymsfield, S. B., Heo, M., Jebb, S. A., Murgatroyd, P. R., & Sakamoto, Y. (2000). Healthy percentage body fat ranges: An approach for developing guidelines based on body mass index. *American Journal of Clinical Nutrition*, *72*(3). <https://doi.org/10.1093/ajcn/72.3.694>
- Geyer, H. J., Schramm, K.-W., Damerud, P. O., Aune, M., Feicht, A., Fried, K. W., Henkelmann, B., Lenoir, D., Schmid, P., & McDonald, T. a. (2004). Terminal Elimination Half-Lives of the Brominated Flame Retardants TBBPA, HBCD, and Lower Brominated PBDEs in Humans. *Organohalogen Compd*, *66*, 3820–3825.
- Ginsberg, G., Hattis, D., & Sonawane, B. (2004). Incorporating pharmacokinetic differences between children and adults in assessing children's risks to environmental toxicants. *Toxicol Appl Pharmacol*, *198*(2), 164–183. <https://doi.org/10.1016/j.taap.2003.10.010>
- Hays, S. M., Aylward, L. L., LaKind, J. S., Bartels, M. J., Barton, H. A., Boogaard, P. J., Brunk, C., DiZio, S., Dourson, M., Goldstein, D. A., Lipscomb, J., Kilpatrick, M. E., Krewski, D., Krishnan, K., Nordberg, M., Okino, M., Tan, Y. M., Viau, C., & Yager, J. W. (2008). Guidelines for the derivation of Biomonitoring Equivalents: Report from the Biomonitoring Equivalents Expert Workshop. *Regul Toxicol Pharmacol*, *51*(3 SUPPL.), S4–S15. <https://doi.org/10.1016/j.yrtph.2008.05.004>
- Hays, S. M., Becker, R. A., Leung, H. W., Aylward, L. L., & Pyatt, D. W. (2007). Biomonitoring equivalents: A screening approach for interpreting biomonitoring results from a public health risk perspective. *Regul Toxicol Pharmacol*, *47*(1), 96–109. <https://doi.org/10.1016/j.yrtph.2006.08.004>
- Hays, S. M., Pyatt, D. W., Kirman, C. R., & Aylward, L. L. (2012). Biomonitoring Equivalents for benzene. *Regul Toxicol Pharmacol*, *62*(1), 62–73. <https://doi.org/10.1016/j.yrtph.2011.12.001>

- Hendriks, A. J., Smítková, H., & Huijbregts, M. A. J. (2007). A new twist on an old regression: Transfer of chemicals to beef and milk in human and ecological risk assessment. *Chemosphere*, *70*(1), 46–56. <https://doi.org/10.1016/j.chemosphere.2007.07.030>
- Hertelyova, Z., Salaj, R., Chmelarova, A., Dombrovsky, P., Dvorakova, M. C., & Kruzliak, P. (2016). The association between lipid parameters and obesity in university students. *Journal of Endocrinological Investigation*, *39*(7). <https://doi.org/10.1007/s40618-015-0240-8>
- Judson, R. S., Kavlock, R. J., Setzer, R. W., Cohen Hubal, E. A., Martin, M. T., Knudsen, T. B., Houck, K. A., Thomas, R. S., Wetmore, B. A., & Dix, D. J. (2011). Estimating toxicity-related biological pathway altering doses for high-throughput chemical risk assessment. In *Chem Res Toxicol* (Vol. 24, Issue 4, pp. 451–462). <https://doi.org/10.1021/tx100428e>
- Kelly, B. C., Gobas, F. A. P. C., & McLachlan, M. S. (2004). Intestinal absorption and biomagnification of organic contaminants in fish, wildlife, and humans. In *Environ Toxicol Chem* (Vol. 23, Issue 10, pp. 2324–2336). <https://doi.org/10.1897/03-545>
- Kerger, B. D., Leung, H. W., Scott, P., Paustenbach, D. J., Needham, L. L., Patterson, D. G., Gerthoux, P. M., & Mocarelli, P. (2006). Age- and concentration-dependent elimination half-life of 2,3,7,8-tetrachlorodibenzo-p-dioxin in Seveso children. *Environ Health Perspect*, *114*(10). <https://doi.org/10.1289/ehp.8884>
- Kirman, C. R., Aylward, L. L., Hays, S. M., Krishnan, K., & Nong, A. (2011). Biomonitoring Equivalents for DDT/DDE. *Regul Toxicol Pharmacol*, *60*(2), 172–180. <https://doi.org/10.1016/j.yrtph.2011.03.012>
- Krishnan, K., Adamou, T., Aylward, L. L., Hays, S. M., Kirman, C. R., & Nong, A. (2011). Biomonitoring Equivalents for 2,2',4,4',5-pentabromodiphenylether (PBDE-99). *Regul Toxicol Pharmacol*, *60*(2), 165–171. <https://doi.org/10.1016/j.yrtph.2011.03.011>
- Krishnan, K., Gagné, M., Nong, A., Aylward, L. L., & Hays, S. M. (2010). Biomonitoring Equivalents for bisphenol A (BPA). *Regul Toxicol Pharmacol*, *58*(1), 18–24. <https://doi.org/10.1016/j.yrtph.2010.06.005>
- Kuga, K., Ito, K., Chen, W., Wang, P., & Kumagai, K. (2020). A numerical investigation of the potential effects of e-cigarette smoking on local tissue dosimetry and the deterioration of indoor air quality. *Indoor Air*, *30*(5), 1018–1038. <https://doi.org/10.1111/ina.12666>
- Kyle, U. G., Schutz, Y., Dupertuis, Y. M., & Pichard, C. (2003). Body composition interpretation: Contributions of the fat-free mass index and the body fat mass index. *Nutrition*, *19*(7–8). [https://doi.org/10.1016/S0899-9007\(03\)00061-3](https://doi.org/10.1016/S0899-9007(03)00061-3)
- La Merrill, M., Emond, C., Kim, M. J., Antignac, J. P., Le Bizec, B., Clément, K., Birnbaum, L. S., & Barouki, R. (2013). Toxicological function of adipose tissue: Focus on persistent organic pollutants. In *Environ Health Perspect* (Vol. 121, Issue 2). <https://doi.org/10.1289/ehp.1205485>
- LaKind, J. S., & Naiman, D. Q. (2008). Bisphenol A (BPA) daily intakes in the United States: Estimates from the 2003-2004 NHANES urinary BPA data. *J Expo Sci Environ Epidemiol*, *18*(6), 608–615. <https://doi.org/10.1038/jes.2008.20>
- Li, D., Sangion, A., & Li, L. (2020). Evaluating consumer exposure to disinfecting chemicals against coronavirus disease 2019 (COVID-19) and associated health risks. *Environ Int*, *145*, 106108. <https://doi.org/10.1016/j.envint.2020.106108>
- Li, L., Arnot, J. A., & Wania, F. (2018). Revisiting the Contributions of Far- and Near-Field Routes to Aggregate Human Exposure to Polychlorinated Biphenyls (PCBs). *Environ Sci Technol*, *52*(12), 6974–6984. <https://doi.org/10.1021/acs.est.8b00151>
- Li, L., Arnot, J. A., & Wania, F. (2019). How are Humans Exposed to Organic Chemicals Released to Indoor Air? *Environ Sci Technol*, *53*(19), 11276–11284. <https://doi.org/10.1021/acs.est.9b02036>
- Li, L., Hoang, C., Arnot, J. A., & Wania, F. (2019). Clarifying Temporal Trend Variability in

- Human Biomonitoring of Polybrominated Diphenyl Ethers through Mechanistic Modeling. *Environ Sci Technol*, 166–175. <https://doi.org/10.1021/acs.est.9b04130>
- Li, L., & Wania, F. (2017). Mechanistic Pharmacokinetic Modeling of the Bioamplification of Persistent Lipophilic Organic Pollutants in Humans during Weight Loss. *Environ Sci Technol*, 51(10), 5563–5571. <https://doi.org/10.1021/acs.est.7b00055>
- Li, L., Westgate, J. N., Hughes, L., Zhang, X., Givehchi, B., Toose, L., Armitage, J. M., Wania, F., Egeghy, P., & Arnot, J. A. (2018). A Model for Risk-Based Screening and Prioritization of Human Exposure to Chemicals from Near-Field Sources. *Environ Sci Technol*, 52(24), 14235–14244. <https://doi.org/10.1021/acs.est.8b04059>
- Li, L., Zhang, Z., Men, Y., Baskaran, S., Sangion, A., Wang, S., Arnot, J., & Wania, F. (2022). Retrieval, Selection, and Evaluation of Chemical Property Data for Assessments of Chemical Emissions, Fate, Hazard, Exposure, and Risks. *ACS Environ Au*, 2(5), 376–395. <https://doi.org/10.1021/acsenvironau.2c00010>
- Liao, K. H., Tan, Y. M., & Clewell, H. J. (2007). Development of a screening approach to interpret human biomonitoring data on volatile organic compounds: Reverse dosimetry on biomonitoring data for trichloroethylene. *Risk Anal*, 27(5), 1223–1236. <https://doi.org/10.1111/j.1539-6924.2007.00964.x>
- Louisse, J., Beekmann, K., & Rietjens, I. M. C. M. (2017). Use of physiologically based kinetic modeling-based reverse dosimetry to predict in vivo toxicity from in vitro data. In *Chem Res Toxicol* (Vol. 30, Issue 1, pp. 114–125). <https://doi.org/10.1021/acs.chemrestox.6b00302>
- Mackay, D. (2001). Multimedia environmental models: The fugacity approach, second edition. In *Multimedia Environmental Models: The Fugacity Approach, Second Edition*. <https://doi.org/10.1201/9781420032543>
- Mackay, D., Celsie, A. K. D., & Parnis, J. M. (2015). The evolution and future of environmental partition coefficients. In *Environ Rev* (Vol. 24, Issue 1, pp. 101–113). <https://doi.org/10.1139/er-2015-0059>
- Macleod, M., Scheringer, M., & Hungerbühler, K. (2007). Estimating enthalpy of vaporization from vapor pressure using Trouton's rule. *Environ Sci Technol*, 41(8), 3249–3253. <https://doi.org/10.1021/es0608186>
- Mage, D. T., Allen, R. H., Gondy, G., Smith, W., Barr, D. B., & Needham, L. L. (2004). Estimating pesticide dose from urinary pesticide concentration data by creatinine correction in the Third National Health and Nutrition Examination Survey (NHANES-III). In *J Expo Anal Environ Epidemiol* (Vol. 14, Issue 6, pp. 457–465). <https://doi.org/10.1038/sj.jea.7500343>
- Mangoni, A. A., & Jackson, S. H. D. (2004). Age-related changes in pharmacokinetics and pharmacodynamics: Basic principles and practical applications. In *Br J Clin Pharmacol* (Vol. 57, Issue 1, pp. 6–14). <https://doi.org/10.1046/j.1365-2125.2003.02007.x>
- Mansouri, K., Grulke, C. M., Judson, R. S., & Williams, A. J. (2018). OPERA models for predicting physicochemical properties and environmental fate endpoints. *J Cheminformatics*, 10(1). <https://doi.org/10.1186/s13321-018-0263-1>
- Martinez, M. N., & Amidon, G. L. (2002). A mechanistic approach to understanding the factors affecting drug absorption: A review of fundamentals. *Journal of Clinical Pharmacology*, 42(6), 620–643. <https://doi.org/10.1177/00970002042006005>
- Milbrath, M. O. G., Wenger, Y., Chang, C. W. C. W., Emond, C., Garabrant, D., Gillespie, B. W., & Jolliet, O. (2009). Apparent half-lives of dioxins, furans, and polychlorinated biphenyls as a function of age, body fat, smoking status, and breast-feeding. In *Environ Health Perspect* (Vol. 117, Issue 3). <https://doi.org/10.1289/ehp.11781>
- Moser, G. A., & McLachlan, M. S. (2002). Modeling digestive tract absorption and desorption of lipophilic organic contaminants in humans. *Environ Sci Technol*, 36(15), 3318–3325.

- <https://doi.org/10.1021/es0158531>
- O'Connor, I. A., Huijbregts, M. A. J., Ragas, A. M. J., & Hendriks, A. J. (2013). Predicting the oral uptake efficiency of chemicals in mammals: Combining the hydrophilic and lipophilic range. *Toxicology and Applied Pharmacology*, 266(1), 150–156. <https://doi.org/10.1016/j.taap.2012.10.015>
- Orive, G., Lertxundi, U., Brodin, T., & Manning, P. (2022). Greening the Pharmacy. *Science*, 377(6603), 259–260. <https://doi.org/10.1126/science.abp9554>
- Partosch, F., Mielke, H., Stahlmann, R., Kleuser, B., Barlow, S., & Gundert-Remy, U. (2015). Internal threshold of toxicological concern values: enabling route-to-route extrapolation. *Arch Toxicol*, 89(6), 941–948. <https://doi.org/10.1007/s00204-014-1287-6>
- Paul Friedman, K., Gagne, M., Loo, L. H., Karamertzanis, P., Netzeva, T., Sobanski, T., Franzosa, J. A., Richard, A. M., Lougee, R. R., Gissi, A., Lee, J. Y. J., Angrish, M., Dorne, J. Lou, Foster, S., Raffaele, K., Bahadori, T., Gwinn, M. R., Lambert, J., Whelan, M., ... Thomas, R. S. (2020). Utility of in Vitro Bioactivity as a Lower Bound Estimate of in Vivo Adverse Effect Levels and in Risk-Based Prioritization. *Toxicol Sci*, 173(1), 202–225. <https://doi.org/10.1093/toxsci/kfz201>
- Pearce, R. G., Setzer, R. W., Strobe, C. L., Sipes, N. S., & Wambaugh, J. F. (2017). Httk: R package for high-throughput toxicokinetics. *Journal of Statistical Software*, 79. <https://doi.org/10.18637/jss.v079.i04>
- Pepelko, W. E., & Withey, J. R. (1985). Methods for route-to-route extrapolation of dose. *Toxicology and Industrial Health*, 1(4), 153–170. <https://doi.org/10.1177/074823378500100410>
- Perbellini, L., Princivale, A., Cerpelloni, M., Pasini, F., & Brugnone, F. (2003). Comparison of breath, blood and urine concentrations in the biomonitoring of environmental exposure to 1,3-butadiene, 2,5-dimethylfuran, and benzene. *Int Arch Occup Environ Health*, 76(6), 461–466. <https://doi.org/10.1007/s00420-003-0436-7>
- Research Triangle Institute. (2005). Methodology for Predicting Cattle Biotransfer Factors. *US Environmental Protection Agency*. <https://archive.epa.gov/epawaste/hazard/tsd/td/web/pdf/btfreportfull05.pdf> (Accessed August 01, 2022).
- Ring, C. L., Arnot, J. A., Bennett, D. H., Egeghy, P. P., Fantke, P., Huang, L., Isaacs, K. K., Jolliet, O., Phillips, K. A., Price, P. S., Shin, H. M., Westgate, J. N., Setzer, R. W., & Wambaugh, J. F. (2019). Consensus Modeling of Median Chemical Intake for the U.S. Population Based on Predictions of Exposure Pathways. *Environ Sci Technol*, 53(2), 719–732. <https://doi.org/10.1021/acs.est.8b04056>
- Rotroff, D. M., Wetmore, B. A., Dix, D. J., Ferguson, S. S., Clewell, H. J., Houck, K. A., LeCluyse, E. L., Andersen, M. E., Judson, R. S., Smith, C. M., Sochaski, M. A., Kavlock, R. J., Boellmann, F., Martin, M. T., Reif, D. M., Wambaugh, J. F., & Thomas, R. S. (2010). Incorporating human dosimetry and exposure into high-throughput in vitro toxicity screening. *Toxicol Sci*, 117(2), 348–358. <https://doi.org/10.1093/toxsci/kfq220>
- Shirai, J. H., & Kissel, J. C. (1996). Uncertainty in estimated half-lives of PCBs in humans: Impact on exposure assessment. *Sci Total Environ*, 187(3), 199–210. [https://doi.org/10.1016/0048-9697\(96\)05142-X](https://doi.org/10.1016/0048-9697(96)05142-X)
- Szczygielska, A., Widomska, S., Jaraszkiwicz, M., Knera, P., & Muc, K. (2003). Blood lipids profile in obese or overweight patients. *Annales Universitatis Mariae Curie-Skłodowska. Sectio D: Medicina*, 58(2).
- Tan, Y. M., Liao, K. H., & Clewell, H. J. (2007). Reverse dosimetry: Interpreting trihalomethanes biomonitoring data using physiologically based pharmacokinetic modeling. *J Expo Sci*

- Environ Epidemiol*, 17(7), 591–603. <https://doi.org/10.1038/sj.jes.7500540>
- Travis, C. C., & Arms, A. D. (1988). Bioconcentration of Organics in Beef, Milk, and Vegetation. *Environ Sci Technol*, 22(3), 271–274. <https://doi.org/10.1021/es00168a005>
- U.S. Environmental Protection Agency. (2012). *Estimation Programs Interface (EPI) Suite for Microsoft® Windows (ver 4.11)* (4.11). U.S. Environmental Protection Agency. <https://www.epa.gov/tsca-screening-tools/epi-suite-estimation-program-interface> (accessed August 01, 2022).
- Varma, M. V. S., Obach, R. S., Rotter, C., Miller, H. R., Chang, G., Steyn, S. J., El-Kattan, A., & Troutman, M. D. (2010). Physicochemical space for optimum oral bioavailability: Contribution of human intestinal absorption and first-pass elimination. *Journal of Medicinal Chemistry*, 53(3), 1098–1108. <https://doi.org/10.1021/jm901371v>
- Wambaugh, J. F., Setzer, R. W., Reif, D. M., Gangwal, S., Mitchell-Blackwood, J., Arnot, J. A., Joliet, O., Frame, A., Rabinowitz, J., Knudsen, T. B., Judson, R. S., Egeghy, P., Vallero, D., & Cohen Hubal, E. A. (2013). High-throughput models for exposure-based chemical prioritization in the ExpoCast project. *Environ Sci Technol*, 47(15), 8479–8488. <https://doi.org/10.1021/es400482g>
- Wambaugh, J. F., Wang, A., Dionisio, K. L., Frame, A., Egeghy, P., Judson, R., & Setzer, R. W. (2014). High throughput heuristics for prioritizing human exposure to environmental chemicals. *Environ Sci Technol*, 48(21), 12760–12767. <https://doi.org/10.1021/es503583j>
- Wambaugh, J. F., Wetmore, B. A., Pearce, R., Strobe, C., Goldsmith, R., Sluka, J. P., Sedykh, A., Tropsha, A., Bosgra, S., Shah, I., Judson, R., Thomas, R. S., & Setzer, R. W. (2015). Toxicokinetic triage for environmental chemicals. *Toxicol Sci*, 147(1), 55–67. <https://doi.org/10.1093/toxsci/kfv118>
- Wang, Z., Walker, G. W., Muir, D. C. G., & Nagatani-Yoshida, K. (2020). Toward a Global Understanding of Chemical Pollution: A First Comprehensive Analysis of National and Regional Chemical Inventories. *Environ Sci Technol*, 54(5), 2575–2584. <https://doi.org/10.1021/acs.est.9b06379>
- Wei, W., Ramalho, O., & Mandin, C. (2020). Modeling the bioaccessibility of inhaled semivolatile organic compounds in the human respiratory tract. *Int J Hyg Environ Health*, 224, 113436. <https://doi.org/10.1016/j.ijheh.2019.113436>
- Wetmore, B. A. (2015). Quantitative in vitro-to-in vivo extrapolation in a high-throughput environment. *Toxicology*, 332, 94–101. <https://doi.org/10.1016/j.tox.2014.05.012>
- Wong, F., Cousins, I. T., & MacLeod, M. (2013). Bounding uncertainties in intrinsic human elimination half-lives and intake of polybrominated diphenyl ethers in the North American population. *Environ Int*, 59, 168–174. <https://doi.org/10.1016/j.envint.2013.05.004>
- Wynne, H. A., Cope, L. H., Mutch, E., Rawlins, M. D., Woodhouse, K. W., & James, O. F. W. (1989). The effect of age upon liver volume and apparent liver blood flow in healthy man. *Hepatology*, 9(2), 297–301. <https://doi.org/10.1002/hep.1840090222>
- Zhang, Z., Wang, S., & Li, L. (2021). Emerging investigator series: The role of chemical properties in human exposure to environmental chemicals. In *Environ Sci Process Impacts* (Vol. 23, Issue 12, pp. 1839–1862). <https://doi.org/10.1039/d1em00252j>

Appendices

Appendix 1 – Description of the PROTEX’s exposure and toxicokinetic module used in this work:

The PROTEX’s one-compartmental exposure and toxicokinetic module is detailed in Li et al. (L. Li, Arnot, et al., 2018) and briefed here. Based on the fugacity approach, the module calculates the accumulation of chemicals as the mass balance between flows of chemical absorption (“Abs”) through ingestion, inhalation, and dermal routes (with subscripts “ING”, “INH”, and “D”, respectively) and flows of elimination (“Elim”) through exhalation, egestion, urination, biotransformation, and percutaneous excretion (with subscripts “R”, “E”, “U”, “B”, and “P”, respectively), namely,

$$\begin{aligned} \frac{dM_{\text{body}}}{dt} &= \frac{d(BV_{\text{eff}} \cdot Z_{\text{body}} \cdot f)}{dt} \\ &= Abs_{\text{ING}} + Abs_{\text{INH}} + Abs_{\text{D}} - Elim_{\text{R}} - Elim_{\text{E}} - Elim_{\text{U}} - Elim_{\text{B}} \\ &\quad - Elim_{\text{P}} \end{aligned}$$

where, the product of the “effective” body volume (BV_{eff} ; i.e., the summed volumes of neutral storage lipids, phospholipids, proteins, and water in the human body) (L. Li & Wania, 2017), the fugacity capacity of the human body (Z_{body} ; see Appendix 2), and chemical fugacity in the human body (f), represents the total amount of a chemical within the human body (M_{body}). This module is parameterized with age- and bodyweight-dependent physiological factors (see Appendix 2 and 3) and chemical-specific partition coefficients and biotransformation half-lives (see Appendix 2).

This work focuses on chemical absorption through the ingestion and inhalation routes. PROTEX calculates the flow of chemical absorption as the product of an intestinal or respiratory “absorption efficiency” (AE ; i.e., the fraction passing the absorption barrier; for details of calculation, see Appendix 4) and the dose of intake (assumed to be 1 $\mu\text{g}/\text{d}$ in this case), namely,

$$Abs_{(\text{ING or INH})} = AE_{(\text{ING or INH})} \times \text{Dose}_{(\text{ING or INH})}.$$

On the other hand, the flow of chemical elimination is quantified as the product of the chemical fugacity in the human body (f) and corresponding transfer “D-value” (for details of calculation, see Appendix 2), following the fugacity approach, namely,

$$Elim_{(\text{R, E, U, B, or P})} = D_{(\text{R, E, U, B, or P})} \times f.$$

Appendix 2 – Quantification of chemical elimination from the human body:

PROTEX quantifies the following five major routes through which chemicals are eliminated from the human body: (L. Li, Arnot, et al., 2018)

(1) Exhalation

PROTEX expresses chemical elimination through exhalation for a certain age (expressed as a D-value $D_{R,age}$) as a function of the rate of respiration ($R_{respiration,age,weight}$ in m^3/h ; age- and bodyweight-dependent):

$$D_{R,age} = R_{respiration,age,weight} \times Z_{air}$$

whereby Z_{air} is the fugacity capacity of the exhaled air.

(2) Egestion

PROTEX quantifies chemical elimination through egestion for a certain age (expressed as a D-value $D_{E,age}$), assuming that the rate of fecal excretion is 10% of the total rate of food ingestion ($R_{food,age,weight}$ in m^3/h ; age- and bodyweight-dependent): (Moser & McLachlan, 2002)

$$D_{E,age} = 10\% \times R_{food,age,weight} \times Z_{feces}$$

whereby Z_{feces} is the fugacity capacity of human feces.

(3) Urination

PROTEX quantifies chemical elimination through urination for a certain age (expressed as a D-value $D_{U,age}$), by considering the renal clearance by glomerular filtration (with an age- and bodyweight-dependent rate $GFR_{age,weight}$ in m^3/h) of the protein-unbound fraction of chemicals (f_{ub} , unitless), as well as renal tubular reabsorption (f_{reabs} ; unitless): (Mackay, 2001)

$$D_{U,age} = GFR_{age,weight} \times f_{ub} \times (1 - f_{reabs}) \times Z_{blood}$$

whereby Z_{blood} is the fugacity capacity of the blood. The calculation of f_{ub} and f_{reabs} follows Armitage et al. (Armitage et al., 2021)

(4) Biotransformation

PROTEX quantifies hepatic biotransformation of chemicals for a certain age (expressed as a D-value $D_{B,age}$), using a whole-body biotransformation half-life (HL_{bio} in h) corresponding to the “effective” body volume (BV_{eff} in m^3) corrected for the reduced metabolism capability for individuals aged >50 ($CORR_{E,age}$ is 1 for ages 0 to 50 and declines linearly to 0.25 at age 90): (Mangoni & Jackson, 2004; Wynne et al., 1989)

$$D_{B,age} = \frac{\ln 2}{HL_{bio}} \times BV_{eff} \times Z_{body} \times CORR_{E,age}$$

whereby Z_{body} is the fugacity capacity of the human body.

(5) Percutaneous excretion

PROTEX expresses chemical elimination through percutaneous lipid excretion for a certain age (expressed as a D-value $D_{P,age}$) as a function of the rate of skin desquamation ($R_{desquamation,age}$ in m^3/h ; age-dependent):

$$D_{P,age} = R_{desquamation,age} \times Z_{skin}$$

Whereby Z_{skin} is the fugacity capacity of the skin.

The above calculations involve the fugacity capacities of air, feces, blood, the human

body, and skin, which are expressed as the linear combinations of the fugacity capacities of fundamental phases such as air (Z_{air}), water (Z_{water}), neutral storage lipids (Z_{nlipid}), phospholipids (Z_{plipid}), and proteins (Z_{protein}), weighted by their respective volume fractions (v ; Appendix 5-Table A.1). That is, for fundamental phases, we have (Endo et al., 2011; L. Li et al., 2022; Mackay, 2001)

$$\begin{aligned} Z_{\text{air}} &= \frac{1}{R \times T_{\text{body}}} \\ Z_{\text{water}} &= \frac{Z_{\text{air}}}{K_{\text{AW}}} \\ Z_{\text{nlipid}} &= K_{\text{nlipid-water}} \times Z_{\text{water}} = K_{\text{OW}} \times Z_{\text{water}} \\ Z_{\text{plipid}} &= K_{\text{plipid-water}} \times Z_{\text{water}} = 1.32 \times K_{\text{OW}}^{1.01} \times Z_{\text{water}} \\ Z_{\text{protein}} &= K_{\text{protein-water}} \times Z_{\text{water}} = 0.41 \times K_{\text{OW}}^{0.73} \times Z_{\text{water}} \end{aligned}$$

whereby, K_{AW} is the air-water partition coefficient, and K_{OW} is the octanol-water partition coefficient, calculated by $K_{\text{OA}} \times K_{\text{AW}}$.

For feces, blood, human body, and skin, we have:

$$\begin{aligned} Z_{\text{feces}} &= Z_{\text{nlipid}} \times v_{\text{nlipid,feces}} + Z_{\text{water}} \times v_{\text{water,feces}} \\ Z_{\text{blood}} &= Z_{\text{nlipid}} \times v_{\text{nlipid,bld}} + Z_{\text{plipid}} \times v_{\text{plipid,bld}} + Z_{\text{protein}} \times v_{\text{protein,bld}} \\ &\quad + Z_{\text{water}} \times v_{\text{water,bld}} \\ Z_{\text{body}} &= Z_{\text{nlipid}} \times v_{\text{nlipid,body}} + Z_{\text{plipid}} \times v_{\text{plipid,body}} + Z_{\text{protein}} \times v_{\text{protein,body}} \\ &\quad + Z_{\text{water}} \times v_{\text{water,body}} \\ Z_{\text{skin}} &= Z_{\text{nlipid}} \times v_{\text{nlipid,skin}} + Z_{\text{plipid}} \times v_{\text{plipid,skin}} + Z_{\text{protein}} \times v_{\text{protein,skin}} \\ &\quad + Z_{\text{water}} \times v_{\text{water,skin}} \end{aligned}$$

Appendix 3 – Calculation of blood and urinary concentrations of chemicals:

Blood: Solving the module equations in Appendix 1 gives an estimate of the chemical fugacity in the human body (f), which can be then combined with the fugacity capacity of blood (Z_{blood} ; see Appendix 2) to calculate the blood concentration of a chemical, namely,

$$C_B = f \times Z_{\text{blood}}.$$

Urine: The urinary concentration of a chemical is calculated by dividing the chemical flow excreted through urination ($N_{U,age}$) by the urine flow (R_{age}), where

$$N_{U,age} = D_{U,age} \times F_U$$

that is,

$$N_{U,age} = GFR_{age,weight} \times f_{ub} \times (1 - f_{reabs}) \times Z_{blood} \times F_U$$

and

$$R_{age} = GFR_{age,weight} \times (1 - f_{reabs})$$

Therefore, the urinary concentration can be calculated as

$$C_U = \frac{N_{U,age}}{R_{age}} = f_{ub} \times Z_{blood} \times F_U$$

Appendix 4 – Quantification of intestinal and respiratory absorption efficiencies:

(1) The calculation of the intestinal absorption efficiency follows the model by Moser and MaLachlan (Moser & McLachlan, 2002). Briefly, this approach describes chemical mass balance in the digestive tract by considering (i) advective transport of chemicals in the intestine through dietary intake and fecal excretion, and (ii) diffusive transport of chemicals across water and lipid (approximated by octanol) films between the intestine and the rest of the body. Here, the fecal excretion process depends on the rate of fecal excretion, which is assumed to be 10% of the age- and bodyweight-dependent total rate of food ingestion ($R_{\text{food,age,weight}}$), as described in Appendix 2. Therefore, our calculated intestinal absorption efficiency is also age- and bodyweight-dependent. Since the original model is a steady-state model, our calculation represents the steady-state intestinal absorption efficiency under constant, continuous dietary intake.

(2) The calculation of the respiratory absorption efficiency is based on the model by Wei et al. (Wei et al., 2020) Briefly, this approach considers the movement of gas- and particle-phase of chemicals in the head, tracheobronchial, and alveolar regions, each of which further comprises a gas phase, a particle phase, and a mucus phase. For each region, this approach describes chemical mass balance in the respiratory tract by considering (i) advective transport to the previous (exhalation) and subsequent (inhalation) regions, (ii) diffusive transport between the gas phase and mucus and between the gas phase and particle phase, and (iii) deposition of particle phase of chemicals. This approach assumes absorption takes place in the alveolar region only. We further assume that the fraction of chemicals distributed in the alveolar mucus phase and absorbed by the alveolar epithelium along with mucus (with a bodyweight-normalized rate of mucus absorption of $11 \text{ L/h/kgBW}^{0.75}$, taken from Clewell et al. (Clewell et al., 2001)), represents the respiratory absorption efficiency, given that the absorption efficiency was not defined in the original model. Here, the advective transport depends on the rate of respiration ($R_{\text{respiration,age,weight}}$), which is age- and bodyweight-dependent. In addition, the original model is a dynamic model providing time-variant predictions, here we calculate the steady-state respiratory absorption efficiency to be consistent with the intestinal absorption efficiency.

Appendix 5 – Table A.1: Comparison of modeled dose-to-concentration ratios (DCRs, in L/d) with DCRs calculated based on literature-reported data:

	DCR _{blood}		DCR _{urine}	
	Literature-reported	Predicted	Literature-reported	Predicted
HBCDs ⁽¹⁾	4.8	64		
Hexachlorobenzene ⁽²⁾	0.43	25		
p,p'-DDT ⁽³⁾	0.064	22		
2,2',4,4',5-PentaBDE ⁽⁴⁾	0.0034	22		
2,4-D ⁽⁵⁾			0.018	0.0033
Benzene ⁽⁶⁾	2977	13256	2653	25367
Bisphenol A ⁽⁷⁾	2359	7258		
Oxytetracycline dihydrate ⁽⁸⁾	392	57659		
Triclosan ⁽⁹⁾	24-121	1141		
Parathion ⁽¹⁰⁾	1414	288		

Notes:

(1) Calculated based on a human-equivalent POD of 38,000 ng/g lipid (converted to 146.87 mg/L based on a conversion factor of 3.865 kg-lipid/L-blood predefined in PROTEX) and an ingested point of departure (POD) of 10 mg/kg/d (converted to 700 mg/d, assuming the generic human bodyweight of 70 kg) (Aylward & Hays, 2011). Here the general body weight of 70 kg was used because it was the weight used in the cited paper. This number is also similar to the bodyweight of 71 kg predefined within PROTEX for a 25-year-old average American woman. The paper derived the DCR based on a lipid basis concentration assuming distribution of the chemical only in body lipid and a whole-body half-life.

(2) Calculated based on a BE of 3384 ng/g lipid (converted to 13.08 mg/L based on a conversion factor of 3.865 kg-lipid/L-blood predefined in PROTEX) and an ingested point of departure (POD) of 0.08 mg/kg/d (converted to 5.6 mg/d, assuming the generic human bodyweight of 70 kg) (Aylward et al., 2010). The BE was derived based on the interspecies extrapolation of concentrations observed within rats fed with a given dose of hexachlorobenzene.

(3) Calculated based on a BE of 14 mg/kg lipid (converted to 54.11 mg/L based on a conversion factor of 3.865 kg-lipid/L-blood predefined in PROTEX) and an ingested point of departure (POD) of 0.05 mg/kg-d (converted to 3.5 mg/d, assuming the generic human bodyweight of 70 kg) (Kirman et al., 2011). The BE was derived based on the interspecies extrapolation of concentrations observed within rats fed with a given dose of DDT.

(4) Calculated based on a BE of 51.6 mg/kg lipid (converted to 200 mg/L based on a conversion factor of 3.865 kg-lipid/L-blood predefined in PROTEX) and an ingested human-equivalent point of departure (POD) of 0.0097 mg/kg/d (converted to 0.679 mg/d, assuming the generic human bodyweight of 70 kg) (Krishnan et al., 2011). The BE paper derived the DCR based on an overestimated lipid basis concentration that is derived from half-life of 2.9 years (taken from Geyer et al (Geyer et al., 2004)), which was then evaluated by Wong et al (Wong et al., 2013) to “underestimate” the whole-body half-life because of a lack of intake rate or exposure pathway understanding and possible PBDE congeners within the body that have not been considered.

(5) Calculated based on a human-equivalent BE_{pod} of 20,000 ug/L (converted to 20 mg/L) and an ingested Chronic RfD of 0.005 mg/kg/d (converted to 0.35 mg/d, assuming the generic human bodyweight of 70 kg) (Aylward & Hays, 2008). The BE was derived based on the interspecies extrapolation of concentrations observed within rats fed with a given dose of 2,4-D.

(6) Calculated based on a BE of 4.4 ug/L (converted to 0.0044 mg/L) for blood and 4.9 ug/L (converted to 0.0049 mg/L) for urine and an inhaled point of departure (POD) of 0.9 mg/m³ (converted to 13.1 mg/d, assuming generic daily inhalation rate to be 14.5 m³/day) (Hays et al., 2012). The BE for blood was derived through the use of a pre-developed PBPK model (E. A. Brown et al., 1998) while the BE for urine was derived through the use of a benzene blood to urine relationship (Perbellini et al., 2003).

(7) Calculated based on the steady state plasma concentration of 0.13 uM calculated by a PBPK model assuming 1mg/kg/day intake dose (converted to 70 mg/day assuming the generic human body weight of 70 kg) (Rotroff et al., 2010).

(8) Calculated based on the steady state plasma concentration of 0.36 uM calculated by a PBPK model assuming 1mg/kg/day intake dose (converted to 70 mg/day assuming the generic human body weight of 70 kg) (Rotroff et al., 2010).

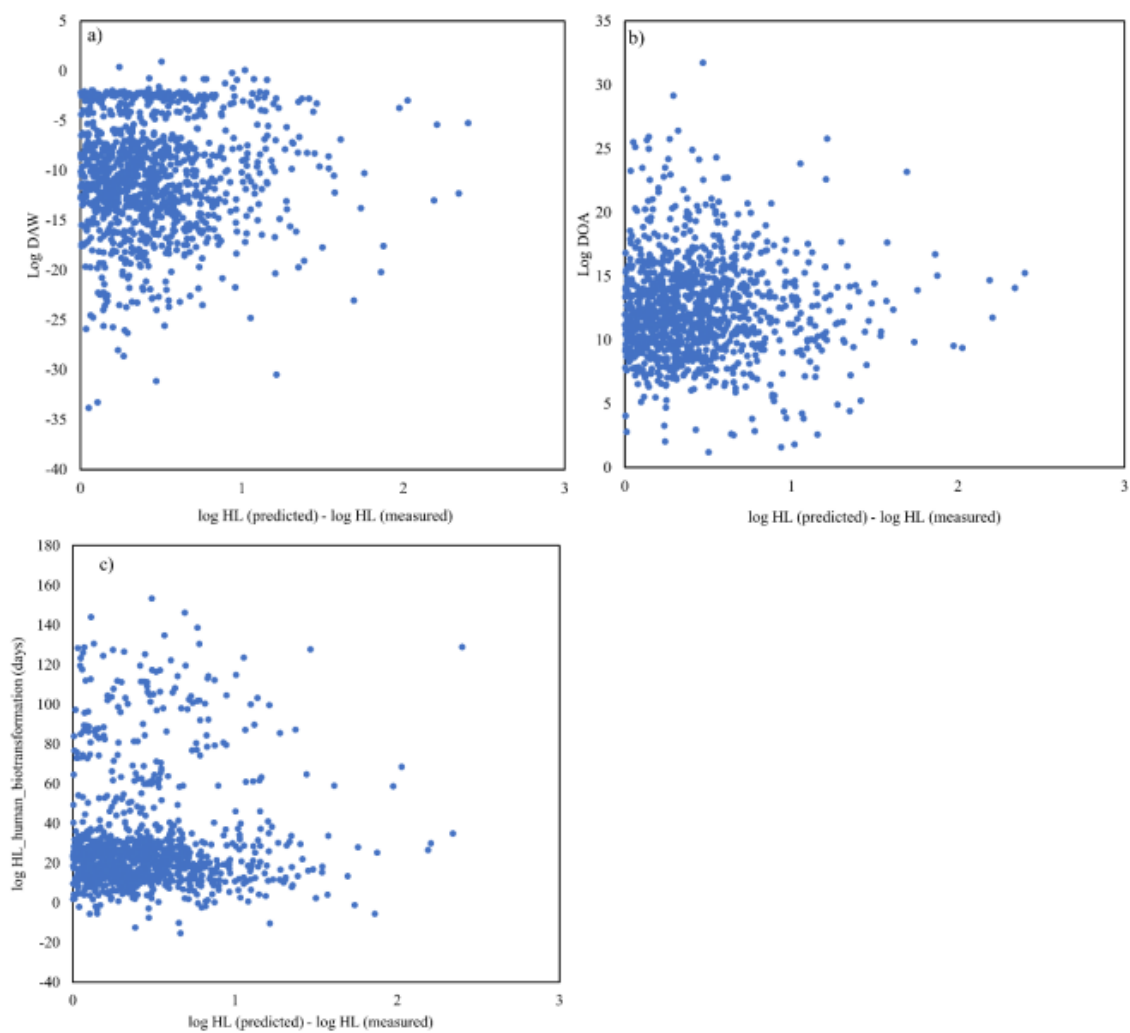
(9) Calculated based on the steady state plasma concentration of 2-10 uM calculated by a PBPK model assuming 1mg/kg/day intake dose (converted to 70 mg/day assuming the generic human body weight of 70 kg) (Rotroff et al., 2010).

(10) Calculated based on the steady state plasma concentration of 0.17 uM calculated by a PBPK model assuming 1mg/kg/day intake dose (converted to 70 mg/day assuming the generic human body weight of 70 kg) (Rotroff et al., 2010).

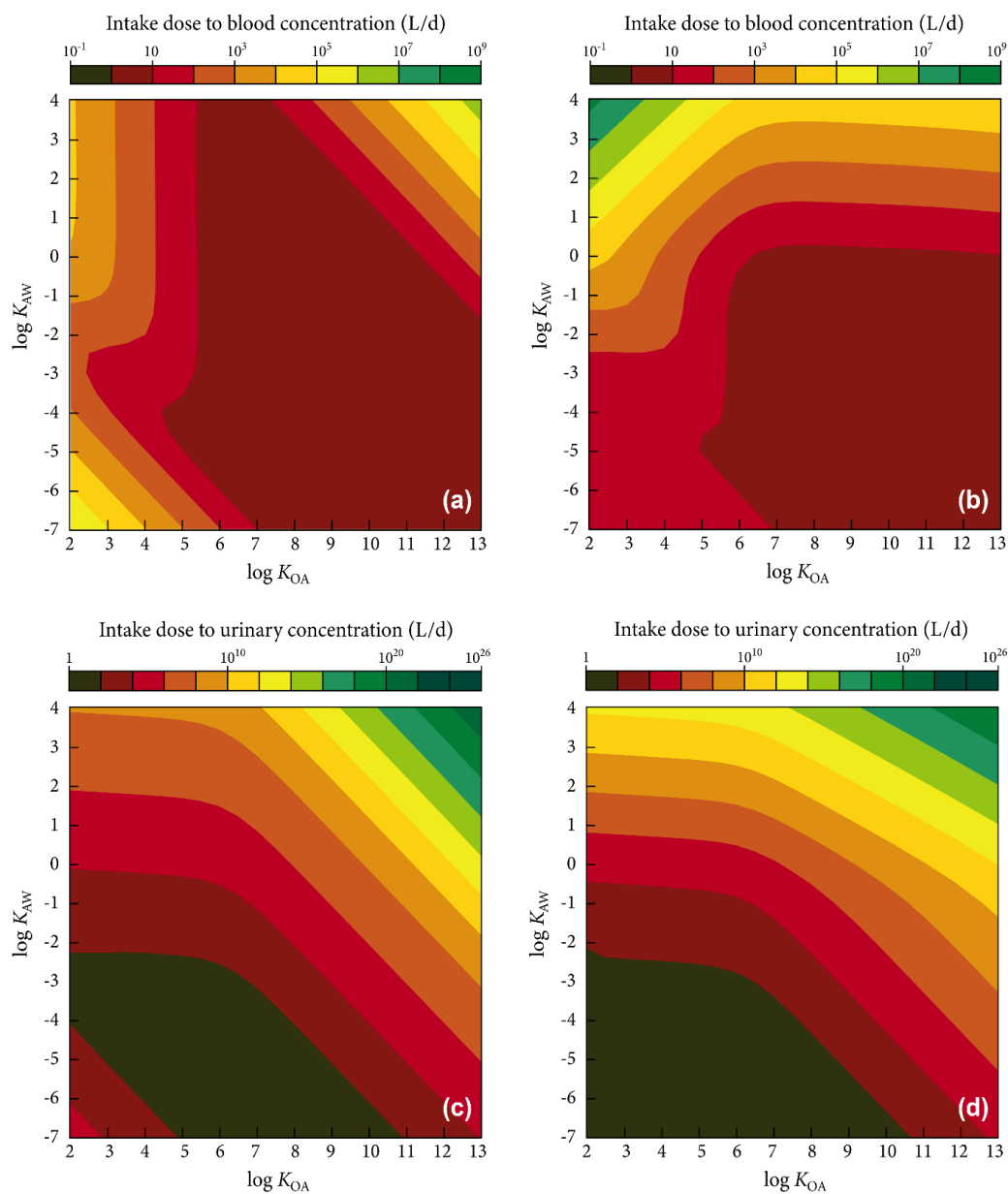
Additional comment: Here we exclude a study on the BE of bisphenol A, where DCR_{urine} was calculated to be 1.8 L/d, based on a urinary BE of 20 mg/L and an ingested human-equivalent point of departure (POD) of 0.5 mg/kg/d (converted to 35 mg/d, assuming the generic human bodyweight of 70 kg) (Krishnan et al., 2010). This DCR_{urine} is very different from our predicted DCR of 262,408. When calculating urinary BE, Ref. (Krishnan et al., 2010) follows Lakind and Naiman (LaKind & Naiman, 2008) to assume 100% ingested absorption and 100% elimination of BPA

through urination, without considering the biotransformation of BPA. We believe this assumption leads to a substantial underestimation of DCR_{urine} , given that BPA has a fairly short biotransformation half-life (~ 7 h), and that biotransformation cannot be ignored.

Appendix 6 – Figure A.1: The relationship between the model's residual (namely the difference between predicted and measured half-lives) and chemical properties D_{AW} = Air-water distribution coefficient; D_{OA} = Octanol-air distribution coefficient; HL = human biotransformation half-life:



Appendix 7 – Figure A.2: Chemical partitioning space illustrating the ratio of intake dose to blood concentration for ingestion (Panel a) and inhalation (Panel b), as well as the ratio of intake dose to urinary concentration for ingestion (Panel c) and inhalation (Panel d), of hypothetical perfectly persistent chemicals (molar mass = 300 g/mol), by an archetypal 3-year-old female American child. Chemicals are arranged by $\log K_{AW}$ and $\log K_{OA}$; diagonals represent chemicals with equal $\log K_{OW}$.



Appendix 8 – Figure A.3: Chemical partitioning space illustrating the ratio of intake dose to blood concentration for ingestion (Panel a) and inhalation (Panel b), as well as the ratio of intake dose to urinary concentration for ingestion (Panel c) and inhalation (Panel d), of hypothetical perfectly persistent chemicals (molar mass = 300 g/mol), by a 25-year-old female American who has twice bodyweight of an average female American. Chemicals are arranged by $\log K_{AW}$ and $\log K_{OA}$; diagonals represent chemicals with equal $\log K_{OW}$.

